

Transfer Learning with Partially Observable Offline Data via Causal Bounds

Xueping Gong, Wei You, and Jiheng Zhang

Department of Industrial Engineering and Decision Analytics

The Hong Kong University of Science and Technology

Abstract

Transfer learning has emerged as an effective approach to accelerate learning by integrating knowledge from related source agents. However, challenges arise due to data heterogeneity – such as differences in feature sets or incomplete datasets – which often results in the nonidentifiability of causal effects. In this paper, we investigate transfer learning in partially observable contextual bandits, where agents operate with incomplete information and limited access to hidden confounders. To address the challenges posed by unobserved confounders, we formulate optimization problems to derive tight bounds on the nonidentifiable causal effects. We then propose an efficient method that discretizes the functional constraints of unknown distributions into linear constraints, allowing us to sample compatible causal models through a sequential process of solving linear programs. This approach takes into account estimation errors and exhibits strong convergence properties, ensuring robust and reliable causal bounds. Leveraging these causal bounds, we improve classical bandit algorithms, achieving tighter regret upper and lower bounds relative to the sizes of action sets and function spaces. In tasks involving function approximation, which are crucial for handling complex context spaces, our method significantly improves the dependence on function space size compared to previous work. We formally prove that our causally enhanced algorithms outperform classical bandit algorithms, achieving notably faster convergence rates. The applicability of our approach is further illustrated through an example of offline pricing policy learning with censored demand. Simulations confirm the superiority of our approach over state-of-the-art methods, demonstrating its potential to enhance contextual bandit agents in real-world applications, especially when data is scarce, costly, or restricted due to privacy concerns.

1 Introduction

Bandit learning problems involve an agent making a series of decisions to maximize rewards or minimize regrets (Lattimore and Szepesvári 2020). Traditional bandit algorithms typically operate without prior knowledge. With the abundance of data collected from various sources, transfer learning has emerged as a powerful tool to accelerate learning by leveraging knowledge from a related source agent, as discussed in Zhuang et al. (2020). Most transfer learning methods assume that both the source and target agents have access to the same complete information (Cai et al. 2024, Liu et al. 2018). Often, the data available from the source and target agents differ in features,

or completeness. This heterogeneity poses a challenge when transferring knowledge because the information isn't directly compatible. We address this challenge by focusing on transfer learning in partially observable contextual bandit (POCB) problems. In this setting, an agent makes a series of decisions (such as choosing an action based on current context) to maximize rewards, but both the source and target agents have access to possibly different and incomplete sets of information.

Transfer learning in POCB has practical applications for integrating knowledge from heterogeneous data sources. For example, in training personalized recommendation systems for e-commerce platforms, the source agent learns from detailed website user behavior (full context), while the target agent focuses on mobile app users who provide only partial data due to privacy restrictions or technical limitations. New influencing factors may also emerge that were absent in earlier data, making datasets from different periods or platforms heterogeneous. A similar challenge arises in autonomous driving systems. The source agent gathers data from human drivers, including sensor readings like steering angle and environmental conditions. However, human decision-making involves cognitive processes that cannot be captured by sensors. The target agent aims to develop autonomous vehicles capable of making safe and efficient decisions but faces heterogeneity because the context of human decision-making is only partially observable. These examples highlight the need for effective knowledge transfer across heterogeneous datasets.

In the presence of heterogeneous data, transfer learning becomes more challenging. In POCB, agents have access only to partial contextual information, which complicates the task of accurately estimating the rewards of actions using source data. Previous works (Bilaj et al. 2023, Chen et al. 2023, Gong and Zhang 2023, Islam et al. 2022, Nikolaev et al. 2013, Zhang and Bareinboim 2021) have attempted to address this issue by introducing additional assumptions, such as the availability of proxy variables or predefined causal relationships between observed and unobserved information. While these approaches can be effective, the assumptions they rely on are often impractical in real-world scenarios, which limits their applicability. In the absence of such assumptions, transferring knowledge from a source domain can sometimes degrade the performance of the target model, leading to what is known as *negative transfer* (Rosenstein et al. 2005).

To address these challenges, it is crucial to focus on causal effects, which capture the intrinsic properties of the environment and remain invariant across domains (e.g., (Bareinboim et al. 2015, Cai et al. 2024, Eberhardt et al. 2024, Lattimore et al. 2016, Liu et al. 2021)). However, identifying causal effects is often hindered by uncertainties in the underlying causal models, which creates a significant barrier to the effective application of transfer learning. Moreover, most existing works on offline transfer learning rely on the availability of instrumental variables (IVs) or proxies to infer causal relationships. As highlighted by Kallus (2018), Xu et al. (2021), obtaining such variables is often challenging or infeasible in many applications.

In this paper, we adopt the structural causal model framework (Pearl and Mackenzie 2018). Our approach distills information from the source agent into causal bounds that are guaranteed to encapsulate the true causal effects of actions on rewards. By leveraging these bounds, we reduce inefficient exploration in bandit algorithms, thereby accelerating learning and ensuring faster convergence to optimal policies. The bounds are derived from optimization problems that identify feasible causal effects compatible with the partially observed offline data, allowing us to effectively transfer knowledge even when direct identification is hindered by unobserved confounding variables.

Solving the proposed optimization problem is nontrivial due to its nonconvexity. To address

this, we introduce an innovative sampling method that generates random samples from the feasible set of causal models compatible with the observed data. This method relies on sequentially solving linear programs, significantly improving efficiency. Our sampling algorithms naturally incorporate estimation and approximation errors by introducing linear constraints to account for these uncertainties.

Our contributions.

We introduce new tight causal bounds for partially observable transfer learning algorithms and develop efficient sampling algorithms that sequentially solve refined linear programming problems to compute these bounds. Under mild assumptions on the sampling distribution, we prove that the ordered statistics generated by our algorithms converge in probability to the bounds obtained from discretized optimization problems. With the assistance of an optimization oracle, this convergence is strengthened to almost sure convergence. Importantly, our algorithms handle estimation errors and continuous variables—areas often neglected in previous literature (Li and Pearl 2022, Liu et al. 2021, Zhang and Bareinboim 2021). More importantly, our methods require transferring only a few causal bounds rather than entire datasets, which is particularly beneficial in privacy-sensitive applications.

Our causal bounds approach is broadly applicable to various causal models and target causal effects, making it a versatile tool for transfer learning applications that extend beyond POCB. To demonstrate, we apply our framework to offline pricing policy learning with censored demand in Section 5.

We provide theoretical guarantees that our proposed algorithms outperform existing ones, as summarized in Table 4. Our results explicitly characterize how transfer learning impacts gap-dependent and minimax regrets in terms of bandit quantities. We extend our approach by incorporating function approximation for continuous context spaces. Our regret analysis demonstrates an improvement in dependence on the policy space Π from $\sqrt{|\Pi|}$ to $\sqrt{\log |\Pi|}$ compared with Zhang and Bareinboim (2021). Our method accommodates general reward functions, greatly expanding the scope compared with existing methods (Tennenholtz et al. 2021), which heavily rely on the linear structure of rewards. These theoretical guarantees are further confirmed by numerical experiments.

Related works.

Our work is related to research on causal bounds. The do-calculus introduced by Pearl (2009) identifies causal effects using probabilistic tools, while Tian and Pearl (2002) derived model-free causal bounds for non-identifiable problems. Linear programming approaches for obtaining causal bounds in discrete settings were proposed by Zhang and Bareinboim (2017) and made scalable by Shridharan and Iyengar (2022). Extensions to non-binary outcomes and continuous variables were explored by Li and Pearl (2024a,b), Zhang and Bareinboim (2021) using instrumental variables. However, these LP-based methods may not yield tight bounds and often rely on structural assumptions about hidden confounders. To address partially observable back-door and front-door criteria, Li and Pearl (2022) employed nonlinear optimization to compute causal bounds. Although effective, solving such nonlinear problems is computationally intensive and can get trapped in lo-

cal optima. Duarte et al. (2024) provided an automated approach for causal inference in discrete settings, summarizing these optimization-based methods. Zhang et al. (2022) used Markov Chain Monte Carlo (MCMC) methods to approximate causal bounds with observational data, which rely on structural assumptions about latent confounders.

Our work is closely related to transfer learning. Previous studies have investigated transfer learning in multi-armed bandit problems (Lazaric et al. 2013, Zhang and Bareinboim 2017), contextual bandits with covariate shift where tasks share the same reward function (Cai et al. 2024), and reinforcement learning settings (Liu et al. 2021). Similarly, Tennenholtz et al. (2021) enhance online learning in linear bandits using a partially missing offline dataset. We extend the framework of Tennenholtz et al. (2021) to general reward functions using our proposed adaptive inverse gap weighting technique. While several papers (Park and Faradonbeh 2021) investigate POCB, few focus on transfer learning within this setting. Transfer learning methods also have broad applications in operations management, including offline pricing policy learning (Bu et al. 2020, Ren et al. 2024, Tang et al. 2022).

Partially Observable Markov Decision Process (POMDP), including general partially observable dynamical systems (Uehara et al. 2022), share similarities with our setting. Researchers have developed various methods to address causal inference challenges in POMDP. For instance, Guo et al. (2022) use instrumental variables to identify causal effects, while Lu et al. (2023), Shi et al. (2022) extend this approach to incorporate general proxy variables in offline policy evaluation. In online reinforcement learning, Jin et al. (2020), Wang et al. (2021) apply the backdoor criterion to explicitly adjust for confounding bias when confounders are fully observable. These works also incorporate uncertainty from partially observable confounders into the Bellman equation and demonstrate provably optimal learning with linear function approximation in both fully or partially observable datasets. Despite these advancements, transfer learning in POMDP with general function approximation remains an open problem due to the complexity of reinforcement learning. We study POCB with general function approximation, showing its potential to generalize to POMDP and related settings. Additionally, Bian et al. (2024) model offline pricing-policy learning with inventory control within the MDP framework. While existing literature (Buckman et al. 2020, Jin et al. 2021, Yu et al. 2020) has relaxed the full coverage assumption for offline data, Bian et al. (2024) introduce partial observability in the MDP setting, where certain price points may be absent from the offline dataset.

Organization.

The rest of the paper is organized as follows. Section 2 introduces transfer learning problems in POCB and discusses the inherent challenges. In Section 3, we formally present a sampling method for computing causal bounds. Section 4 leverages these tight causal bounds to enhance transfer learning in POCB. We further demonstrate the application of our framework to offline pricing learning with censored demand in Section 5. In Section 6, we present our numerical results. While we outline proof techniques throughout the paper, complete details are provided in Appendix C.

2 Preliminaries

Throughout the paper, we use capital letters to denote variables (e.g., X) and lowercase letters for their values (e.g. x). Calligraphic fonts, such as \mathcal{X} , to denote the domain of X , with $|\mathcal{X}|$ denoting its cardinality if X is finite and discrete. The cumulative distribution function of the random variable X is represented by $F(x)$, and the corresponding empirical distribution is denoted as $\hat{F}(x)$.

2.1 Causal models and identifiability

We use structural causal models (SCMs, Pearl and Mackenzie 2018) as the foundational semantic framework for our analysis. SCMs combine the graphical structure of causal diagrams with mathematical functions to describe how variables influence one another. An SCM \mathcal{M} consists of a set of endogenous variables (variables determined within the model) and exogenous variables (external, unobserved variables). The *causal diagram* associated with an SCM is a directed acyclic graph where nodes represent the endogenous variables, and directed edges indicate direct causal effects between them. Exogenous variables are typically not depicted explicitly in the graph; their influence is incorporated via the noise terms in the structural equations. Each endogenous variable is defined by a *structural equation*, which specifies its value as a function of its direct causes (parent variables in the causal diagram) and (possibly) an exogenous noise term. This formalizes the causal dependencies among variables.

In this paper, we focus on the SCM illustrated in Figure 1, which serves as an abstraction of our transfer learning problem in POCB. Here, we denote the observed context variable by W , the unobserved context variable by U , the action variable by A , and the reward variable by Y . The causal relationships among these variables are represented by directed edges in the graph, allowing for an arbitrary causal relationship between W and U . The action A is generated by a policy that depends on W and U ; thus, there are edges from W and U to A . The reward Y is influenced by both context variables and the action; therefore, there are edges from W , U and A to Y . This causal diagram captures the dependencies in our model.

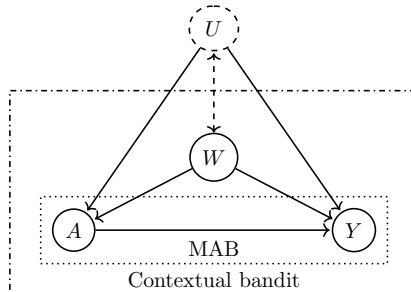


Fig. 1: The causal diagram \mathcal{G} for transfer learning problem in POCB. The dashed double arrow between U and W represents an arbitrary causal relationship. MAB considers only the nodes A and Y (and only the edges between them). When including only nodes A , Y , and W , the diagram represents a CB.

A central task in causal inference is to estimate the effect of an *intervention* on a variable of interest. In particular, the *do-operator* in causal inference, denoted as $\text{do}(A = a)$, represents a hypothetical operation where the action variable A is set to a specific value a through external intervention, rather than by its natural causal dependencies within the system (e.g., in Figure 1,

the observed A is typically determined by (W, U)). The intervention $\text{do}(A = a)$ simulates physical manipulation by modifying the structural causal model: it replaces the structural equation for A with the constant $A = a$, while keeping the rest of the model unchanged. Graphically, this corresponds to deleting all incoming edges to the variable A in the causal diagram, effectively severing its dependence on its usual causes, and leaving the remaining graph intact.

The distribution resulting from this intervention is denoted as $F(y|\text{do}(A = a))$ representing the distribution of the outcome Y after intervening on A . The expected value of Y under this interventional distribution is referred to as the *casual effect*, denoted as $\mathbb{E}_{\mathcal{M}}[Y|\text{do}(A = a)]$. Sometimes, we focus on the conditional causal effect given additional variables, such as $\mathbb{E}_{\mathcal{M}}[Y|\text{do}(A = a), w]$ and $\mathbb{E}_{\mathcal{M}}[Y|\text{do}(A = a), w, u]$.

If all endogenous variables are observed, the causal effect can be uniquely determined from the observational data using the rules of do-calculus (Pearl 2009). However, when some variables are unobserved, the causal effect may not always be identifiable from the data. Let \mathfrak{D} denote the set of observed variables in the causal diagram \mathcal{G} , e.g., $\mathfrak{D} = \{A, Y, W\}$ in Figure 1. For any joint distribution $F(\cdot)$, let $F(\mathfrak{D})$ denote the marginal distribution over \mathfrak{D} . When $F(\cdot)$ represents the distribution of all endogenous variables in the SCM generating the observed data, we refer to $F(\mathfrak{D})$ as the *observational distribution*. We say that an SCM \mathcal{M} is *compatible* with the observational distribution if $F_{\mathcal{M}}(\mathfrak{D})$ matches the observational distribution.

Definition 2.1 (*Identifiability*). *Given an observational distribution $F(\mathfrak{D})$ and a causal diagram \mathcal{G} , a causal effect (e.g., $\mathbb{E}_{\mathcal{M}}[Y|\text{do}(A = a)]$) is said to be identifiable if it remains the same in all SCMs with causal diagram \mathcal{G} that are compatible with $F(\mathfrak{D})$.*

In plain terms, a causal effect is non-identifiable if there exist two SCMs that generate the same observational distribution but yield different values for the causal effect of interest. The identifiability of causal effects can be systematically determined using do-calculus (Pearl 2009). For completeness, we refer readers to Appendix D for a brief review of do-calculus.

2.2 Motivating examples and challenges

In this section, we present motivating examples and highlight challenges in transfer learning tasks under incomplete observational data.

Example 1: using partially observable offline dataset to warm-start online learning. Imagine a healthcare system where offline data has been collected from historical patient records. This dataset includes partially observable information: patients’ health outcomes Y , the treatment administered A and observed contexts W (e.g., age, weight, baseline health conditions). However, critical information such as genetic markers or specific health risk factors (denoted by U), is unobserved due to limitations in past testing or incomplete records. Additionally, some features may be intentionally masked to protect patient privacy. This expansion of the feature set or censoring of sensitive attributes results in a partially observable dataset, summarized as an empirical distribution $\hat{F}(a, y, w)$ of (A, Y, W) .

Example 2: Autonomous driving. Consider the task of training an autonomous driving system. During data collection, an autonomous vehicle (the *agent*) is operated by a human driver (the *expert*), capturing the driving action A , the reward Y (e.g., driving safety), and context variables

W (e.g., radar signals). However, the expert’s judgment of the environment, represented by U , cannot be directly observed by the vehicle’s sensors during learning. The sensor data is thus summarized again as $\hat{F}(a, y, w)$.

The examples above illustrate how incomplete information and unobserved factors can hinder an agent’s ability to learn and perform effectively. We now identify key challenges posed by missing confounders and discuss how causal inference techniques can help address these issues.

Challenge 1: Unobserved confounding impedes reward estimation.

In Example 1, missing features in the offline datasets hinder direct estimation of the true reward function. Previous work by Tennenholtz et al. (2021) addressed this challenge in the linear setting by representing partially observable, confounded data as linear constraints for the online problem. However, in our case, we cannot rely on specific structures or assumptions about the reward functions, as the structural equation for Y may be arbitrary. Similarly, Zhang and Bareinboim (2021) address the general function space by incorporating instrumental variables. Nonetheless, identifying suitable instrumental variables remains an open research problem, and we note that their method does not guarantee optimal regret.

Challenge 2: Negative transfer.

In Example 2, the unobserved expert context U can act as a confounder, influencing both the action A and the reward Y . Using partial observational data on (A, Y, W) generated by the expert – without understanding the expert context U – can lead to negative transfer.

The complication arises from two distinct quantities: the conditional expectation $\mathbb{E}[Y|a, w]$ and the causal effect $\mathbb{E}[Y|\text{do}(A = a), w]$. Naive transfer methods often rely on estimating the conditional expectation as a proxy for the causal effect. However, this approach is biased by the unknown expert policy that generated the offline data. The following example illustrates how such a naive approach can result in a policy that significantly deviates from the optimal one, ultimately causing performance degradation in transfer learning.

Example. Consider a 2-arm contextual bandit problem, where the action A , and context variables U and W are binary. At the beginning of each round, two binary context variables, U and W , are sampled from independent Bernoulli distributions, with $\mathbb{P}(U = 1) = 0.9$ and $\mathbb{P}(W = 1) = 0.5$. The context variables U, W influence the reward Y received in each round, as shown in Table 1.

The expert agent observes the contextual variables U and W and executes a context-aware optimal policy $\pi_{\text{expert}}^* : \mathcal{W} \times \mathcal{U} \rightarrow \mathcal{A}$. Consequently, the expert generates multiple data points, resulting in an observational distribution $\mathbb{P}(A, W)$ as shown in Table 2. With probability 0.9 (i.e., $U = 1$ occurs), π_{expert}^* will select the arm 1. We now proceed to compute the causal effect as follows:

$$\begin{aligned} \mathbb{E}[Y|\text{do}(A = 0), w] &= 10 \times 0.1 + 0.9 \times 0.9 = 1.81, \quad \text{and} \\ \mathbb{E}[Y|\text{do}(A = 1), w] &= 0 \times 0.1 + 1 \times 0.9 = 0.9, \quad \forall w \in \{0, 1\}. \end{aligned}$$

Therefore, the optimal policy for the agent is $\pi_{\text{agent}}^*(W) = 0$ with probability 1. However, this policy differs significantly from π_{expert}^* as π_{expert}^* primarily selects arm 1.

Upon closer examination, it becomes clear that the asymmetrical probability mass function of the hidden context variable U creates a significant discrepancy between the optimal expert and

agent policies. Specifically, for the frequently occurring context $U = 1$, the rewards of the two arms are relatively similar. In contrast, for the rare context $U = 0$, the rewards differ considerably. If the agent is aware of the distribution of U , it can infer that the observed rewards are likely influenced by the skewness in $F(u)$ and adjust its decision-making accordingly to make optimal choices.

(w, u)	(0, 0)	(1, 0)	(0, 1)	(1, 1)
$\mathbb{E}[Y \text{do}(A = 1), w, u]$	0	0	1	1
$\mathbb{E}[Y \text{do}(A = 0), w, u]$	10	10	0.9	0.9

Table 1: Reward function.

(a, w)	(0, 0)	(0, 1)	(1, 0)	(1, 1)
$\mathbb{P}(a, w)$	0.05	0.05	0.45	0.45

Table 2: Observational distribution.

To illustrate this, we present a simple numerical experiment in Figure 4, showing how negative transfer can occur with a naive knowledge transfer approach. This example underscores the importance of focusing on the causal effect, as it reflects the intrinsic causal structure of the environment. When the causal effect is properly identified and transferred, the agent can enhance performance across various transfer learning tasks.

Challenge 3: Causal non-identifiability.

Arguably, the most significant challenge in transfer learning with incomplete data is the potential non-identifiability of the desired causal effects.

If hypothetically, the full knowledge of $F(a, y, w, u)$ were available for transfer, then the target agent could directly derive the causal effect $\mathbb{E}[Y|\text{do}(A = a), w]$. To see this, note that W and U block the back-door path from A to Y , allowing us to use do-calculus rules and condition on U to fully identify the causal effect $\mathbb{E}[Y|\text{do}(A = a), w]$. Specifically, we can marginalize over (A, Y, W) to obtain the marginal distribution $F(u)$ of U , and compute the conditional expectation $\mathbb{E}[Y|a, w, u]$ to derive the causal effect $\mathbb{E}[Y|\text{do}(A = a), w]$, as shown in Proposition 2.1.

Proposition 2.1 *Given $F(a, y, w, u)$, the causal effect $\mathbb{E}[Y|\text{do}(A = a), w]$ is uniquely identified as*

$$\mathbb{E}[Y|\text{do}(A = a), w] = \int_{u \in \mathcal{U}} \mathbb{E}[Y|a, w, u] dF(u).$$

While do-calculus provides a comprehensive method for identifying causal effects, it cannot construct an identification formula if a query is inherently non-identifiable. For example, consider a more challenging transfer setting where both agents observe only partial information – specifically, actions A , outcomes Y and observable contexts W . In cases of incomplete observational data, the required causal effect may be non-identifiable, allowing us to derive only bounds on the causal effect rather than a precise estimate.

2.3 Transfer learning tasks

To address these challenges, we leverage tools from causal inference. The fundamental idea is that, while correlations between variables may be spurious, causal relationships are transferable due to the shared causal structures depicted in Figure 1 between the expert and the agent.

The examples in the previous section underscore the importance of knowing $F(u)$ in addition to partially observed offline data. Although U is unobserved, its distribution is often known in advance (e.g., in Example 1, if U represents gender, genetic markers, or blood type). By leveraging the distributional information $\hat{F}(u)$ in addition to the observational distribution $\hat{F}(a, y, w)$, the agent can establish tight bounds on the causal effect in cases of causal non-identifiability. These bounds enable the agent to rule out suboptimal actions, thereby accelerating learning and reducing regret.

Online learning problems.

We now frame online learning problems in the context of causal inference.

Multi-armed bandit. In a stochastic multi-armed bandit (MAB) problem, an agent is given an SCM \mathcal{M} with a decision node A representing the arm selection and an outcome variable Y representing the reward; see the dotted box in Figure 1 for an illustration. For each arm $a \in \mathcal{A}$, its expected reward μ_a is the effect of the action $\text{do}(A = a)$, i.e., $\mu_a \triangleq \mathbb{E}[Y|\text{do}(A = a)]$. Let $\mu^* = \max_{a \in \mathcal{A}} \mu_a$ and a^* denote the optimal expected reward and the optimal arm, respectively. At each round $t = 1, 2, \dots, T$, the agent performs an action $\text{do}(A_t = a_t)$ and observes a reward Y_t . The objective of the agent is to minimize the cumulative regret:

$$\text{Reg}(T) = T\mu^* - \sum_{t=1}^T \mathbb{E}[\mu_{a_t}], \quad (1)$$

where the expectation is taken with respect to the randomness of the algorithm.

Contextual bandit. We now describe the contextual bandit (CB) problem within a causal framework. Contextual bandits (Agarwal et al. 2012, Chu et al. 2011, Li et al. 2010) are an extension of multi-armed bandits (MAB), where the expert can observe additional contextual information W associated with the reward Y . An agent for a contextual bandit is given an SCM \mathcal{M} with an observed context variable W , an arm selection node A , and a reward variable Y ; see the dash-dotted box in Figure 1 for an illustration. At each round $t = 1, 2, \dots, T$, the agent can observe a context w_t and performs an action $\text{do}(A_t = a_t)$ based on the context and historical information. For each arm $a \in \mathcal{A}$, the expected reward given context w is defined as $\mu_{a,w} \triangleq \mathbb{E}[Y|\text{do}(A = a), w]$. Let μ_w^* denote the optimal expected reward with respect to context w . The objective of the agent is to minimize the cumulative regret, defined as

$$\text{Reg}(T) = \sum_{t=1}^T \mathbb{E}[\mu_{w_t}^* - \mu_{a_t, w_t} | w_t], \quad (2)$$

where the expectation is taken with respect to the randomness of the algorithm. We refer to this setting as the *partially observable contextual bandit* (POCB) problem.

In the scenario where the agent can observe all contexts W and U during online learning, we modify the realizability assumption as follows to incorporate the influence of context U . We refer to this as the *fully observable contextual bandit* (FOCB) setting. For each arm $a \in \mathcal{A}$, the expected reward is now $\mu_{a,w,u} \triangleq \mathbb{E}[Y|\text{do}(A = a), w, u]$. Let $\mu_{w,u}^*$ denote the optimal expected reward with

respect to context (w, u) . The objective of the agent is to minimize the cumulative regret, defined as

$$\text{Reg}(T) = \sum_{t=1}^T \mathbb{E}[\mu_{w_t, u_t}^* - \mu_{a_t, w_t, u_t} | w_t, u_t], \quad (3)$$

where the expectation is taken with respect to the randomness of the algorithm.

It is worth noting that in the contextual bandit setting, the regret generally scales with $|\mathcal{W}|$ and $|\mathcal{U}|$, as the problem can be framed as a generic reinforcement learning problem. We mitigate this dependence using function approximation methods, as detailed in Section 4.3.

Transfer learning tasks.

We consider the case where all agents operate under the same structural causal model (SCM) \mathcal{M} , as depicted in Figure 1. The agents differ in the information they can observe during the learning process and may also use different policies to generate actions. Notably, beyond the observational distribution, we do not assume knowledge of the policy used by the source agent, as it may depend on an unobserved context U .

Specifically, we focus on data collected by an arbitrary source agent that transfers only¹ the distributions (or their estimations) of (A, Y, W) and U . We are interested in the following transfer learning tasks: **Task 1** with a MAB target agent; **Task 2** with a POCB target agent; and **Task 3** with a FOCB target agent.

Task 1 serves as a baseline, establishing the foundation for our framework, methods, and results. We then extend our approach to show its applicability in Tasks 2 and 3, which share methodological similarities.

3 Tight Bounds on Causal Effects

As highlighted in Section 2.2, directly estimating the reward function, determining the optimal policy, or identifying a unique causal effect is generally infeasible with partial data alone. To overcome these challenges, we propose transforming the partially observed dataset into tight causal bounds. In this section, we present a general framework for obtaining these bounds, using Task 1 as an illustrative example.

3.1 Causal bounds via linear programming

We consider an off-policy learning problem where knowledge is transferred from a POCB agent to a MAB agent (Task 1). At each time step, the POCB agent observes the context W , follows a policy to select an action A and observes the corresponding rewards Y . The experience of the POCB agent is summarized as the joint distribution $\hat{F}(a, y, w)$, which is then provided to the MAB agent together with $\hat{F}(u)$. The MAB agent, being unable to observe W , aims to minimize regret as defined in equation (1) by identifying the action a^* with the highest causal effect $\mu_{a^*} = \mathbb{E}[Y | \text{do}(A = a^*)]$. In

¹If the source agent also transfers full knowledge, including U , the task becomes simpler, as the causal effect can be perfectly identified by Proposition 2.1. Thus, we omit its analysis here.

this section, we establish algorithms to generate valid bounds on μ_a , using the received observational distributions.

To isolate the core idea, we first consider two simplifying assumptions: (1) the observational distributions $F(a, y, w)$ and $F(u)$ are perfectly known; and (2) all relevant random variables – A , Y , W and U – are finite and discrete. We will later relax these assumptions in Section 3.3.

Recall that a key challenge is the non-identifiability of the causal effect $\mathbb{E}[Y|\text{do}(A = a)]$ from incomplete data, due to the unblocked back-door path $A \leftarrow U \rightarrow Y$. This implies that the causal effect of A on Y cannot be estimated without bias, regardless of the sample size.

To obtain tight bounds on the causal effect, we consider the following optimization problem, which seeks to maximize or minimize the causal effect over all SCMs compatible with the observational distributions $F(a, y, w)$ and $F(u)$.

$$\begin{aligned} & \sup / \inf \mathbb{E}_{\mathcal{M}}[Y|\text{do}(A = a)], \\ & \text{s.t. } F_{\mathcal{M}}(a, y, w) = F(a, y, w), \\ & \quad F_{\mathcal{M}}(u) = F(u), \end{aligned} \tag{4}$$

where the sup/inf is taken over all causal models \mathcal{M} with the causal diagram \mathcal{G} . We denote the solutions to (4) as $h(a)$ and $l(a)$ for the supremum and infimum, respectively. Since the optimization is conducted over all compatible causal models, the resulting bounds are guaranteed to be tight. It is worth noting that a necessary and sufficient condition for causal identifiability is that $h(a) = l(a)$. A formal statement of this result is provided in the appendix. This approach is inspired by related works, such as (Pearl 2009, Tian and Pearl 2002, Zhang et al. 2022).

Note that previous works have considered similar optimization problems but often yield non-tight causal bounds. For instance, the solutions from the nonlinear optimization problem in (Li and Pearl 2022) may not correspond to any valid causal model, resulting in non-tight bounds. We observe that focusing solely on constraints for the specific value a of interest generally leads to looser bounds. Therefore, to obtain tight bounds, it is essential to incorporate constraints for *all* $a' \in \mathcal{A}$, rather than just the value a relevant to the intervention $\text{do}(A = a)$.

The original optimization problem (4) is challenging to solve due to inefficiency and intractability. First, the functional constraints on unknown distributions make the optimization problem inherently complex. Second, nonlinear optimization can often get trapped in local optima, and in some cases, narrow causal bounds that fail to encompass the true causal effects may lead to critical misjudgments.

To address these challenges, we note that the optimization problem can be naturally simplified by expressing it in terms of probability mass functions for discrete random variables.

Suppose the domains of the relevant random variables are discrete and partitioned into singleton sets, i.e., $\mathcal{A} = \cup_{i=1}^{n_A} \mathcal{A}_i$, $\mathcal{Y} = \cup_{j=1}^{n_Y} \mathcal{Y}_j$, $\mathcal{W} = \cup_{k=1}^{n_W} \mathcal{W}_k$, $\mathcal{U} = \cup_{l=1}^{n_U} \mathcal{U}_l$. We begin by defining

$$\theta_{ijk} = \int_{a \in \mathcal{A}_i, y \in \mathcal{Y}_j, w \in \mathcal{W}_k} dF(a, y, w), \quad \forall i, j, k, \quad \theta_l = \int_{u \in \mathcal{U}_l} dF(u), \quad \forall l, \tag{5}$$

and

$$x_{ijkl} = \int_{a \in \mathcal{A}_i, y \in \mathcal{Y}_j, w \in \mathcal{W}_k, u \in \mathcal{U}_l} dF_{\mathcal{M}}(a, y, w, u).$$

Integrating both sides of the first constraint in (4) over \mathcal{A}_i , \mathcal{Y}_j , and \mathcal{W}_k to obtain

$$\sum_l x_{ijkl} = \theta_{ijk}.$$

This reformulates the first constraint in terms of integration, replacing the original pointwise equality. For the second constraint in (4), we rewrite it as

$$\int_{a \in \mathcal{A}, y \in \mathcal{Y}, w \in \mathcal{W}} dF_{\mathcal{M}}(a, y, w, u) = F(u), \quad \forall u \in \mathcal{U}.$$

Integrating these constraints over $u \in \mathcal{U}_l$, we get

$$\sum_{ijk} x_{ijkl} = \theta_l.$$

Compared with the original functional constraints on distributions, these linear constraints on x_{ijkl} are far more tractable. Finally, using do-calculus, the objective of the original optimization problem can be reformulated as

$$\mathbb{E}_{\mathcal{M}}[Y | \text{do}(A = a_i)] = \sum_{j,k,l} \frac{y_j x_{ijkl} \sum_{i',j'} x_{i'j'kl}}{\sum_{j'} x_{ij'kl}}. \quad (6)$$

Putting everything together, we can now express the optimization problem in terms of the unknown variables x_{ijkl} as the following nonlinear programming problem

$$\begin{aligned} \max / \min \quad & \sum_{j,k,l} \frac{y_j x_{ijkl} \sum_{i',j'} x_{i'j'kl}}{\sum_{j'} x_{ij'kl}}, \\ \text{s.t.} \quad & \sum_l x_{ijkl} = \theta_{ijk}, \quad \forall i, j, k, \\ & \sum_{i,j,k} x_{ijkl} = \theta_l, \quad \forall l, \\ & 0 \leq x_{ijkl} \leq 1, \quad \forall i, j, k, l. \end{aligned} \quad (7)$$

The transfer learning task involves obtaining causal bounds for each action a , or equivalently, for each index i , resulting in $n_{\mathcal{A}}$ separate optimization problems. This approach, however, becomes inefficient as the number of actions grows. To address this, we propose a sampling method that efficiently solves all optimization problems in a unified manner.

3.2 A sampling method for efficient optimization

Notably, all optimization problems share the same feasible region, suggesting that they can be solved simultaneously. However, naively combining all optimization tasks into a single large-scale optimization problem remains computationally expensive, as the resulting problem is non-convex. To overcome this, we introduce a sampling method that significantly reduces the need for complex optimization procedures. Additionally, this sampling method offers both an intuitive explanation and numerical evidence for why the approach by Li and Pearl (2022) may fail to yield tight bounds, and how our approach improves upon it.

The main idea is to randomly draw samples from the feasible region of the optimization problem (7), which is a polytope defined by $n_{\mathcal{A}}n_{\mathcal{Y}}n_{\mathcal{W}} + n_{\mathcal{U}} - 1$ linearly independent constraints. Given that there are $n_{\mathcal{A}}n_{\mathcal{Y}}n_{\mathcal{W}}n_{\mathcal{U}}$ unknown variables, this setup requires determining the values of $n_{\mathcal{A}}n_{\mathcal{Y}}n_{\mathcal{W}}n_{\mathcal{U}} - n_{\mathcal{A}}n_{\mathcal{Y}}n_{\mathcal{W}} - n_{\mathcal{U}} + 1$ unknowns.

Efficiently sampling probability tables with row and column constraints, however, remains challenging. A naive approach would be to sample each x_{ijkl} independently from a uniform distribution supported on $[0, 1]$, rejecting any samples that do not meet the constraints. This approach can be highly sample-inefficient.

To improve efficiency, we can incorporate inequality constraints to narrow the sampling range and increase the likelihood of generating valid samples.

Given that we are essentially considering all possible joint distributions with fixed marginals, Li and Pearl (2022) used the Fréchet inequalities to reduce the search space for x_{ijkl} , as follows:

$$\max\{0, \theta_{ijk} + \theta_l - 1\} \leq x_{ijkl} \leq \min\{\theta_{ijk}, \theta_l\}. \quad (8)$$

However, the solutions generated by Li and Pearl (2022), which involve sampling each variable from the reduced interval in (8), may not satisfy all the constraints in (7), leading to a lack of tightness.

One may further improve sample efficiency by solving the following *linear programming problem* to find tight bounds on each x_{ijkl} :

$$\begin{aligned} & \max / \min x_{ijkl}, \\ & \text{s.t. linear constraints in (7)}. \end{aligned} \quad (9)$$

While these bounds are tight for each *individual* x_{ijkl} , the Cartesian product of these bounds may not be tight for the entire vector of x_{ijkl} values.

To support this claim, we report the proportion of valid samples (i.e., joint distributions that satisfy the constraints) obtained using different sample spaces in Table 3 for the example discussed in Section 6. We observed that even with the bounds derived from the individual LPs in (9), only 0.3% of the samples were valid, leading to a significant loss in sample efficiency.

sample space for x_{ijkl}	proportion of valid samples
$[0, 1]$	≈ 0
support given by (8)	$< 10^{-4}$
support given by (9)	0.3%
Algorithm 1	100%

Table 3: Proportion of valid samples obtained with different sample spaces for the example in Section 6.

We introduce a sampling algorithm based on sequential linear programming to generate valid samples from the feasible region. Let S denote a set of free variables for the linear equations in (7). The procedure begins by selecting such a set S with cardinality $n_{\mathcal{A}}n_{\mathcal{Y}}n_{\mathcal{W}}n_{\mathcal{U}} - n_{\mathcal{A}}n_{\mathcal{Y}}n_{\mathcal{W}} - n_{\mathcal{U}} + 1$. We then iteratively sample each variable x_{n_r} with $x_{n_r} \in S$. For the first variable x_{n_1} , we solve (9) to determine its support interval $[l_{n_1}, h_{n_1}]$, and then sample a value \hat{x}_{n_1} from a user-specified distribution truncated to $[l_{n_1}, h_{n_1}]$. At iteration r , with the values of $x_{n_1}, \dots, x_{n_{r-1}}$ already sampled,

we add constraints to ensure that each of these variables is fixed to its sampled value. Specifically, we find the support $[l_{n_r}, h_{n_r}]$ for x_{n_r} by solving

$$\begin{aligned} & \max / \min x_{n_r}, \\ & \text{s.t. linear constraints in (7),} \\ & x_{n_s} = \hat{x}_{n_s}, \quad \forall s = 1, 2, \dots, r-1, \end{aligned} \tag{10}$$

We then sample \hat{x}_{n_r} is from the support $[l_{n_r}, h_{n_r}]$. After completing all $|S|$ steps, the remaining $x_{ijkl} \notin S$, can be uniquely determined by solving the equality constraints of (7). With necessary adjustments for continuous variables and estimation error (see Section 3.3), we summarize this sampling algorithm in Algorithm 1.

Each sample represents a possible joint distribution consistent with the observed marginals. By sequentially solving linear programs (LPs), this algorithm ensures that each sample respects the imposed constraints, thereby avoiding invalid distributions and significantly improving sample efficiency; see Table 3 for a comparison with existing methods.

Algorithm 1 Monte-Carlo sampling for compatible causal models using sequential LP

Input: Observational distribution $F(a, y, w)$ and $F(u)$ and sampling distribution F_s

- 1: Select a set of free variables S with cardinality $n_{\mathcal{A}n_{\mathcal{Y}}n_{\mathcal{W}}n_{\mathcal{U}}} - n_{\mathcal{A}n_{\mathcal{Y}}n_{\mathcal{W}}} - n_{\mathcal{U}} + 1$
- 2: Compute each θ_{ijk} and θ_l according to (5)
- 3: Sequentially solve LP (10) to find the support $[l_{ijkl}, h_{ijkl}]$ of x_{ijkl} for each $x_{ijkl} \in S$
- 4: Sample a value \hat{x}_{ijkl} from F_s truncated to $[l_{ijkl}, h_{ijkl}]$ for each $x_{ijkl} \in S$
- 5: Solve the remaining \hat{x}_{ijkl} using the equality constraints in (7) for all $x_{ijkl} \notin S$

Output: Joint distribution of the endogeneous variables represented by $\hat{\mathbf{x}} \triangleq \{\hat{x}_{ijkl} : \forall i, j, k, l\}$

Algorithm 2 utilizes the samples generated by Algorithm 1 to estimate the causal bounds for each action by calculating the smallest and largest ordered statistics.

Algorithm 2 Monte-Carlo estimation for causal bounds in Task 1

Input: Sample size B

- 1: **for** $\tau = 1, 2, \dots, B$ **do**
- 2: Call Algorithm 1 to obtain the sampled causal model $\hat{\mathbf{x}}^\tau$
- 3: For each $a \in \mathcal{A}$, compute the causal effect $b_\tau(a)$ using (6) with $\hat{\mathbf{x}}^\tau$
- 4: For each $a \in \mathcal{A}$, compute $l_B(a) = \min_\tau b_\tau(a)$ and $h_B(a) = \max_\tau b_\tau(a)$

Output: $\{l_B(a), h_B(a) : \forall a \in \mathcal{A}\}$

Under mild assumptions, we have convergence results for the causal bound estimates obtained from Algorithm 2. Let \mathcal{D} denote the feasible region of (7) and let \mathbb{P}_s denote the sampling measure for \mathbf{x} under Algorithm 2. Note that our algorithm guarantees that the support of \mathbb{P}_s belongs to \mathcal{D} .

Proposition 3.1 (Convergence of causal bounds) Assume that the sampling measure \mathbb{P}_s satisfies $\forall \mathbf{x} \in \mathcal{D}$, and $\forall \delta > 0$, $\mathbb{P}_s(\mathcal{B}(\mathbf{x}, \delta) \cap \mathcal{D}) > 0$, where $\mathcal{B}(\mathbf{x}, \delta)$ is a ball centered at \mathbf{x} with radius δ . Then, the outputs of Algorithm 2, $l_B(a)$ and $h_B(a)$, converge in probability to $l(a)$ and $h(a)$ as $B \rightarrow \infty$, respectively.

The condition $\mathbb{P}_s(\mathcal{B}(\mathbf{x}, \delta) \cap \mathcal{D}) > 0$ ensures that the sampling distribution covers all feasible models. This condition can be satisfied by various continuous distributions, such as the uniform distribution, truncated Gaussian distribution, and others.

Remark 3.1 *Similar to Zhang et al. (2022), we can establish a concentration result for our sampling algorithm using Chernoff’s bound. However, this result is not as useful as Proposition 3.1. First, the concentration property depends on the distribution of causal bounds, which is often complex and difficult to determine in practice. Second, when targeting tight causal bounds, convergence results are typically more relevant than concentration results. For example, when several samples for $b_\tau(a)$ are available, the smallest order statistic converges to the true lower bound significantly faster than the average.*

Remark 3.2 *Algorithm 2 can be further refined using an additional optimization procedure. This improves the convergence rate from convergence in probability (Proposition 3.1) to almost sure convergence (Proposition A.1). Detailed implementation and theoretical results are provided in Appendix A.*

3.3 Dealing with estimation error and continuous variables

Causal bounds with estimation error.

Let $\hat{\theta}_l$ and $\hat{\theta}_{ijk}$ represent the estimated values of θ_l and θ_{ijk} , respectively, with corresponding error terms ϵ_l and ϵ_{ijk} . For example, one may use the empirical distributions $\hat{F}(a, y, w)$ and $\hat{F}(u)$ to estimate θ_{ijk} and θ_l as follows:

$$\begin{aligned}\hat{\theta}_{ijk} &= \int_{a \in \mathcal{A}_i, y \in \mathcal{Y}_j, w \in \mathcal{W}_k} d\hat{F}(a, y, w), \forall i \in [n_{\mathcal{A}}], j \in [n_{\mathcal{Y}}], k \in [n_{\mathcal{W}}] \\ \hat{\theta}_l &= \int_{u \in \mathcal{U}_l} d\hat{F}(u), \forall l \in [n_{\mathcal{U}}].\end{aligned}\tag{11}$$

Our framework can seamlessly incorporate these error terms into our sampling method. To account for estimation uncertainty, we introduce the following optimization problem:

$$\begin{aligned}\max_{\mathbf{x}, \boldsymbol{\theta}} / \min_{\mathbf{x}, \boldsymbol{\theta}} & \sum_{j, k, l} \frac{y_j x_{ijkl} \sum_{i', j'} x_{i' j' k l}}{\sum_{j'} x_{i j' k l}}, \\ \text{s.t.} & \sum_{l'} x_{ijkl l'} = \theta_{ijk}, \quad \sum_{i' j' k'} x_{i' j' k' l} = \theta_l, \quad \forall i, j, k, l, \\ & |\theta_l - \hat{\theta}_l| \leq \epsilon_l, \quad |\theta_{ijk} - \hat{\theta}_{ijk}| \leq \epsilon_{ijk}, \quad \forall i, j, k, l \\ & \sum_{i, j, k} \theta_{ijk} = 1, \quad \sum_l \theta_l = 1, \\ & 0 \leq x_{ijkl} \leq 1, \quad 0 \leq \theta_{ijk} \leq 1, \quad 0 \leq \theta_l \leq 1, \quad \forall i, j, k, l.\end{aligned}\tag{12}$$

To obtain a valid causal model that accounts for estimation error, we need to sample points from the feasible region of (12). For this purpose, we introduce Algorithm 7, designed to generate

random samples from a simplex defined by general linear constraints. This general-purpose algorithm requires solving $n_{\mathcal{A}}n_{\mathcal{Y}}n_{\mathcal{W}}n_{\mathcal{U}} + n_{\mathcal{A}}n_{\mathcal{Y}}n_{\mathcal{W}} + n_{\mathcal{U}}$ linear programs sequentially, which may be computationally intensive. To enhance sampling efficiency, we can focus on sampling only the free variables corresponding to a subset of linearly independent equality constraints. The remaining variables can then be determined by solving for them, as done in Algorithm 2.

Dealing with continuous variables.

We now extend our approach to continuous random variables. We start by discretizing the domains into disjoint blocks, i.e., $\mathcal{A} = \cup_{i=1}^{n_{\mathcal{A}}} \mathcal{A}_i$, $\mathcal{Y} = \cup_{j=1}^{n_{\mathcal{Y}}} \mathcal{Y}_j$, $\mathcal{W} = \cup_{k=1}^{n_{\mathcal{W}}} \mathcal{W}_k$, $\mathcal{U} = \cup_{l=1}^{n_{\mathcal{U}}} \mathcal{U}_l$. As the discretization becomes finer – i.e., as the volumes of blocks \mathcal{A}_i , \mathcal{Y}_j , \mathcal{W}_k and \mathcal{U}_l approach zero for all (i, j, k, l) – the approximation error converges to zero for well-behaved distributions. In certain applications, tight causal bounds are essential, making it necessary to account for approximation errors. To address this, we introduce an error term:

$$\epsilon_{ijk} = \frac{1}{2} \left| \max_{a \in \mathcal{A}_i, y \in \mathcal{Y}_j, w \in \mathcal{W}_k} g(a, y, w) - \min_{a \in \mathcal{A}_i, y \in \mathcal{Y}_j, w \in \mathcal{W}_k} g(a, y, w) \right| \text{vol}(\mathcal{A}_i) \text{vol}(\mathcal{Y}_j) \text{vol}(\mathcal{W}_k),$$

where g represents the probability density, and $\text{vol}(\cdot)$ denotes the volume of the blocks. For the approximation error ϵ_l for θ_l , we can compute it in the same way. By introducing this error term, we can handle approximation errors in a manner similar to estimation errors, allowing for greater precision in determining tight causal bounds, see Appendix C.1.

The optimization problem (4) after discretization is exactly the same as the optimization problem for discrete variables under natural discretization in (7). If all relevant random variables are discrete, this discretization is exact. For general random variables, however, it remains an open question whether the optimal value (denoted as $\hat{l}(a)$ and $\hat{h}(a)$, respectively) for the discretized optimization in (7) converge to those of the continuous version in (4) as the discretization becomes finer.

Moreover, we can explicitly account for discretization error by incorporating an error term into the optimization problem, as demonstrated in (12).

4 Transfer Learning via Causal Bounds

In this section, we apply the tight bounds on causal effects derived in Section 3 to accelerate online learning tasks across different transfer learning settings.

4.1 Task 1: transfer to multi-armed bandit

To begin, we consider the transfer learning problem from a POCEB agent to a MAB agent, i.e., Task 1. The key idea is to use causal bounds to truncate the upper confidence bounds (UCBs) in classical bandit algorithms, thereby eliminating suboptimal arms before the algorithm starts.

Consider a MAB agent facing a finite set of arms, i.e., $|\mathcal{A}| < \infty$. The POCEB agent provides offline data from which causal bounds $l(a)$ and $h(a)$ for each arm $a \in \mathcal{A}$ are derived using Algorithm 2. This ensures that the true expected reward $\mu_a = \mathbb{E}[Y | \text{do}(A = a)] \in [l(a), h(a)]$ for each arm a .

The proposed Algorithm 3 modifies the standard UCB algorithm to incorporate causal bounds, which leads to improved performance in a transfer learning setting. First, any arm a for which $h(a) < \max_{i \in \mathcal{A}} l(i)$ is removed, as these arms are guaranteed to be suboptimal. Specifically, for such arms, we have $\mu_a < h(a) < l(a') < \mu_{a'}$ for some $a' \in \mathcal{A}$. We denote the remaining active arms as

$$\mathcal{A}^* \triangleq \left\{ a \in \mathcal{A} : h(a) \geq \max_{i \in \mathcal{A}} l(i) \right\}.$$

Next, the upper confidence bound $U_a(t)$ for each remaining arm is truncated using the causal bound $h(a)$ yielding the truncated UCB $\hat{U}_a(t) = \min\{U_a(t), h(a)\}$. This step is always valid since $\mu_a < h(a)$, hence $h(a)$ is the maximum feasible level of optimism given the causal bound. The algorithm then selects the arm with the highest truncated UCB, observes the reward, and updates the average reward for the chosen arm.

Algorithm 3 Transfer learning for multi-armed bandit

Input: time horizon T and causal bounds $[l(a), h(a)]$ for each arm $a \in \mathcal{A}$

- 1: Remove any arm a for which $h(a) < \max_{i \in \mathcal{A}} l(i)$ to obtain the active arm set \mathcal{A}^*
 - 2: Initialize the empirical mean $\hat{\mu}_a(1) = 0$ and the number of pulls $n_a(1) = 0$
 - 3: **for** $t = 1, \dots, T$ **do**
 - 4: Compute the upper confidence bound $U_a(t) = \min \left\{ 1, \hat{\mu}_a(t) + \sqrt{\frac{2 \log T}{n_a(t)}} \right\}$ for each $a \in \mathcal{A}^*$
 - 5: Compute the truncated UCB $\hat{U}_a(t) = \min\{U_a(t), h(a)\}$ for each $a \in \mathcal{A}^*$
 - 6: Sample the arm $a_t = \operatorname{argmax}_{a \in \mathcal{A}^*} \hat{U}_a(t)$ and observe a reward y_t
 - 7: Update $\hat{\mu}_{a_t}(t+1) = \frac{\hat{\mu}_{a_t}(t) \cdot n_{a_t}(t) + y_t}{n_{a_t}(t)+1}$ and $n_{a_t}(t+1) = n_{a_t}(t) + 1$
 - 8: For each $a \neq a_t$, update $\hat{\mu}_a(t+1) = \hat{\mu}_a(t)$ and $n_a(t+1) = n_a(t)$
-

We upper bound the expected number of pulls for each sub-optimal arm under Algorithm 3.

Theorem 4.1 *For a MAB problem with a finite action set $|\mathcal{A}| < \infty$ and rewards bounded within $[0, 1]$, the number of draws $\mathbb{E}[N_a(T)]$ in Algorithm 3 for any sub-optimal arm $a \neq a^*$ is upper bounded as follows:*

$$\mathbb{E}[N_a(T)] \leq \begin{cases} 0, & \text{if } a \notin \mathcal{A}^*, \text{ i.e., } h(a) < \max_{i \in \mathcal{A}} l(i) \leq \mu^*, \\ \frac{|\mathcal{A}| \pi^2}{6}, & \text{if } a \in \mathcal{A}^* \text{ and } h(a) < \mu^*, \\ \frac{8 \log T}{\Delta_a^2}, & \text{if } a \in \mathcal{A}^* \text{ and } h(a) \geq \mu^*. \end{cases}$$

where $\Delta_a = \mu^* - \mu_a$ is the sub-optimality gap for the arm a .

Theorem 4.1 illustrates the benefits of incorporating causal bounds in transfer learning scenarios, where arms can be categorized based on their optimality gap sizes. Arms that are definitively suboptimal, as indicated by the causal bounds, are removed from consideration entirely, thereby significantly reducing exploration. For arms with large optimality gaps that cannot be fully ruled out by causal bounds, the algorithm pulls each of these only a constant number of times, effectively controlling sample complexity. Finally, the remaining suboptimal arms, denoted as the effective set of arms

$$\widetilde{\mathcal{A}}^* \triangleq \{a \in \mathcal{A} \mid h(a) \geq \mu^*\},$$

has minimal information in their causal bounds. This set represents arms with potential for optimal performance, and thus warrant significant exploration.

A direct implication of Theorem 4.1 is that the algorithm achieves a lower regret rate compared to standard UCB algorithms that do not utilize causal bounds. When the causal information is strong, the algorithm efficiently eliminates suboptimal arms early, focusing exploration on promising candidates and significantly reducing regret. Even in scenarios where causal information is weak and no arms can be distinguished from the optimal arm using causal bounds, the algorithm leverages truncated UCB values. This truncation limits excessive optimism, effectively reducing unnecessary exploration and enhancing overall performance.

As a straightforward corollary of Theorem 4.1, we formally establish the minimax upper bound on the regret achieved by our method.

Corollary 4.1 *For a MAB problem with a finite action set $|\mathcal{A}| < \infty$ and rewards bounded within $[0, 1]$, the regret of Algorithm 3 is upper bounded by*

$$\mathbb{E}[\text{Reg}(T)] \leq \sqrt{8(|\widetilde{\mathcal{A}}^*| - 1)T \log T}.$$

This minimax regret upper bound matches with the lower bound $\Omega(\sqrt{|\widetilde{\mathcal{A}}^*|T})$ up to a logarithm factor for transfer learning settings. Specifically, denote the contextual bandit instances with prior knowledge on bounds $\mu_a \in [l(a), h(a)]$ as

$$\mathfrak{M} = \{\text{MAB instances with } l(a) \leq \mu_a \leq h(a), \forall a \in \mathcal{A}\}.$$

A minimax regret lower bound is given as follows.

Lemma 4.1 *For a MAB problem with a finite action set $|\mathcal{A}| < \infty$ and rewards bounded within $[0, 1]$, and for any algorithm A , there exists an absolute constant $c > 0$ such that when $T > c$, we have*

$$\min_A \sup_{\mathfrak{M}} \text{Reg}(T) \geq \frac{1}{27} \sqrt{(|\widetilde{\mathcal{A}}^*| - 1)T}.$$

4.2 Task 2: transfer to partially observable contextual bandit

We now consider the task of knowledge transfer between two POCB agents. Here, the source agent shares partial model knowledge, specifically the empirical distributions $\hat{F}(a, y, w)$ and $\hat{F}(u)$, with the target agent. Unlike in Task 1, the target agent now has access to the observed context W , but still lacks information about the unobserved context U . The goal of this target agent is to identify the context-dependent optimal arm $a^*(w)$ for each context w and minimize the cumulative regret over time. In this setting, the causal effect $\mu_{a,w} = \mathbb{E}[Y | \text{do}(A = a), w]$ may not be directly identifiable.

We start by considering settings where the context space is discrete. In the following section, we extend our approach to continuous context spaces, where we employ function approximation techniques to handle the added complexity of continuous variables.

Causal bounds.

To obtain bounds on $\mu_{a,w}$, we extend the approach from Section 3 by solving a context-dependent version of the optimization problem (4):

$$\begin{aligned} & \sup / \inf \mathbb{E}_{\mathcal{M}}[Y | \text{do}(A = a), w], \\ & \text{s.t. } F_{\mathcal{M}}(a, y, w) = F(a, y, w), \quad F_{\mathcal{M}}(u) = F(u). \end{aligned} \tag{13}$$

Following the discretization method outlined in Section 3.3, we approximate the optimization problem (13). Upon discretization, the objective becomes

$$\hat{\mathbb{E}}_{\mathcal{M}}[Y | \text{do}(A = a), w] = \sum_{j,l} \frac{y_j \theta_l x_{ijkl}}{\sum_{j'} x_{ij'kl}}, \tag{14}$$

where $\hat{\mathbb{E}}_{\mathcal{M}}[\cdot]$ denotes the expectation under the discretized distribution, and y_j denotes an arbitrary representative value in the block \mathcal{Y}_j .

Algorithm 4 provides causal bounds for discrete contexts, which can be extended across the entire $\mathcal{Y} \times \mathcal{W}$ space through interpolation techniques. Alternatively, in Section 4.3, we employ function approximation methods to directly handle scenarios with continuous context spaces.

Algorithm 4 Monte-Carlo estimation for causal bounds in Task 2

Input: Discretization of the variable domains $\mathcal{A}, \mathcal{Y}, \mathcal{W}, \mathcal{U}$, and sample size B

- 1: **for** $\tau = 1, 2, \dots, B$ **do**
- 2: Call Algorithm 1 to obtain the sampled causal model $\hat{\mathbf{x}}^\tau$
- 3: For each $a \in \mathcal{A}$ and $w \in \mathcal{W}$, compute the causal effect $b_\tau(a, w)$ using (14) with $\hat{\mathbf{x}}^\tau$
- 4: For each $a \in \mathcal{A}$ and $w \in \mathcal{W}$, compute $l_B(a, w) = \min_\tau b_\tau(a, w)$ and $h_B(a, w) = \max_\tau b_\tau(a, w)$

Output: $\{l_B(a, w), h_B(a, w) : \forall a \in \mathcal{A}, w \in \mathcal{W}\}$

Transfer learning.

With Algorithm 4, we can identify bounds $\mu_{a,w} \in [l(a, w), h(a, w)]$ on the true causal effect $\mu_{a,w} = \mathbb{E}[Y | \text{do}(A = a), w]$. We define the set $\mathcal{A}^*(w)$ as follows:

$$\mathcal{A}^*(w) \triangleq \left\{ a \in \mathcal{A} \mid h(a, w) > \max_{i \in \mathcal{A}} l(i, w) \right\}.$$

This set includes actions that could potentially outperform others for a given context w based on the causal bounds and excludes context-action pairs that are definitively suboptimal. Recall that the optimal expected reward for context w is denoted by $\mu_w^* = \max_{a \in \mathcal{A}} \mathbb{E}[Y | \text{do}(A = a), w]$.

The following theorem generalizes the results of Theorem 4.1 to the contextual bandit setting, as MAB is a special case when $|\mathcal{W}| = 1$. This extension allows us to evaluate the benefit of causal bounds in controlling the exploration of suboptimal arms across different contexts. Let $n_{a,w}(t)$ denote the number of pulls of arm a under context w up to time t , and let $\hat{\mu}_{a,w}(t)$ represent the corresponding sample mean.

Algorithm 5 Transfer learning for contextual bandit

Input: time horizon T and causal bound $l(a, w)$ and $h(a, w)$ for each arm-context pair

- 1: **for** $w \in \mathcal{W}$ **do**
 - 2: Remove any arm a for which $h(a, w) < \max_{i \in \mathcal{A}} l(i, w)$ to obtain the active arm set $\mathcal{A}^*(w)$
 - 3: Initialize $\hat{\mu}_{a,w}(1) = 0$ and $n_{a,w}(1) = 0$
 - 4: **for** $t = 1, 2, \dots, T$ **do**
 - 5: Observe the context w_t
 - 6: Compute the UCB $U_{a,w_t}(t) = \min \left\{ 1, \hat{\mu}_{a,w_t}(t) + \sqrt{\frac{\log t}{n_{a,w_t}(t)}} \right\}$ for each $a \in \mathcal{A}^*(w_t)$
 - 7: Compute the truncated UCB $\hat{U}_{a,w_t}(t) = \min \{ U_{a,w_t}(t), h(a, w_t) \}$ for each $a \in \mathcal{A}^*(w_t)$
 - 8: Sample the arm $a_t = \operatorname{argmax}_{a \in \mathcal{A}^*(w_t)} \hat{U}_{a,w_t}(t)$ and observe a reward y_t
 - 9: Update the empirical mean $\hat{\mu}_{a,w_t}(t)$ and the number of pulls $n_{a,w_t}(t)$
-

Theorem 4.2 Consider a contextual bandit problem with a finite action set $|\mathcal{A}| < \infty$ and a finite context set $|\mathcal{W}| < \infty$, and rewards bounded within $[0, 1]$. For any given context $w \in \mathcal{W}$, suppose w occurs for T_w times. Then the conditional expected number of draws $\mathbb{E}[N_a(T_w)]$ in Algorithm 3 for any sub-optimal arm $a \neq a_w^*$ is upper bounded as:

$$\mathbb{E}[N_a(T_w)] \leq \begin{cases} 0, & \text{if } a \notin \mathcal{A}^*(w), \text{ i.e., } h(a, w) < \max_{i \in \mathcal{A}} l(i, w) \leq \mu_w^*, \\ \frac{|\mathcal{A}|\pi^2}{6}, & \text{if } a \in \mathcal{A}^*(w) \text{ and } h(a, w) < \mu_w^*, \\ \frac{8 \log T_w}{\Delta_{a,w}^2} + |\mathcal{A}|, & \text{if } a \in \mathcal{A}^*(w) \text{ and } h(a, w) \geq \mu_w^*. \end{cases}$$

The classical agent, lacking causal bounds, minimizes regret over $|\mathcal{W}|$ independent bandit instances, treating each context $w \in \mathcal{W}$ as a separate problem. Theorem 4.2 demonstrates how incorporating causal bounds improves the efficiency of classical bandit algorithms by significantly limiting the exploration of suboptimal arms. With these bounds, the agent can establish tight constraints on causal effects for each context-action pair, enabling early elimination of certain arms and focusing exploration on the following subset of arms requiring further examination

$$\widetilde{\mathcal{A}}^*(w) \triangleq \{a \in \mathcal{A} | h(a, w) \geq \mu_w^*\}.$$

Theorem 4.3 For a contextual bandit problem with a finite action set $|\mathcal{A}| < \infty$ and a finite context set $|\mathcal{W}| < \infty$, and rewards bounded within $[0, 1]$, the regret of Algorithm 5 satisfies:

$$\limsup_{T \rightarrow \infty} \frac{\mathbb{E}[\operatorname{Reg}(T)]}{\sqrt{T \log T}} \leq \sum_{w \in \mathcal{W}} \sqrt{8(|\widetilde{\mathcal{A}}^*(w)| - 1) \mathbb{P}(W = w)}.$$

The regret bound in this result scales with $\sqrt{|\widetilde{\mathcal{A}}^*(w)|}$ rather than $\sqrt{|\mathcal{A}^*(w)|}$. Although Algorithm 5 does not explicitly eliminate suboptimal arms in $\widetilde{\mathcal{A}}^*(w) - \mathcal{A}^*(w)$, the truncation by causal upper bounds enables the UCB approach to effectively control the number of pulls for these suboptimal arms. This implicit filtering improves sample efficiency, as arms with high upper causal bounds remain prioritized for exploration, reducing the need to explore less promising arms.

Using the Cauchy-Schwarz inequality, we derive the following upper bound for the cumulative regret:

$$\sum_{w \in \mathcal{W}} \sqrt{8(|\widetilde{\mathcal{A}}^*(w)| - 1)\mathbb{P}(W = w)} \leq \sqrt{8 \sum_{w \in \mathcal{W}} (|\widetilde{\mathcal{A}}^*(w)| - 1)}. \quad (15)$$

This inequality reveals that eliminating suboptimal arms enhances the performance of transfer learning.

Denote the contextual bandit instances with prior knowledge $l(a, w)$ and $h(a, w)$ as

$$\mathfrak{M} = \{\text{contextual bandit instances with } l(a, w) \leq \mu_{a,w} \leq h(a, w), \forall a \in \mathcal{A}, \forall w \in \mathcal{W}\}.$$

Theorem 4.4 *Suppose $|\mathcal{A}| < \infty$ and $|\mathcal{W}| < \infty$. Then for any algorithm \mathbf{A} , there exists an absolute constant $c > 0$ such that*

$$\sup_{\mathfrak{M}} \limsup_{T \rightarrow \infty} \frac{\text{Reg}(T)}{\sqrt{T}} \geq \frac{1}{27} \sum_{w \in \mathcal{W}} \sqrt{(|\widetilde{\mathcal{A}}^*(w)| - 1)\mathbb{P}(W = w)}.$$

The lower bound result indicates that Algorithm 4 is near-optimal up to logarithmic terms in T .

Remark 4.1 *(Connection to Dann et al. 2021) Dann et al. (2021) presents gap-dependent regret upper bounds for tabular reinforcement learning (RL) by excluding state-action pairs not visited by an optimal policy. Their regret scales as*

$$\mathcal{O} \left(\sum_{w \in \mathcal{W}} \sum_{a \in \mathcal{A}^*(w)} \frac{\log T}{\Delta_{a,w}} \right).$$

Contextual bandits can be viewed as a special case of general RL by treating each context as a separate state, so their method is also applicable here. However, RL methods seek to optimize over state-action (context-action) pairs, an objective that is not fully realizable in our setup since contexts evolve independently of the actions taken. Consequently, we define regret in the contextual bandit framework relative to a context-dependent optimal action, as specified by (2), rather than pursuing a unified state-action optimization as in standard RL. Tailored specifically to POCB, our approach leverages causal bounds to focus exploration on contextually relevant actions, thereby reducing unnecessary pulls for suboptimal actions within each context. Moreover, Theorem 4.3 suggests that our regret bounds outperform those in Dann et al. (2021) for minimax regret, as the regret in Dann et al. (2021) scales with the right-hand side term of (15).

4.3 Dealing with continuous context space: function approximations

As suggested by Theorem 4.4, the regret of contextual bandit algorithms scales with the size $|\mathcal{W}|$ of the context space. In this section, we address the case where the context space is continuous, requiring function approximation techniques to handle the infinite set of possible contexts. Learning an optimal policy across all contexts is generally infeasible unless the reward function exhibits specific structures, such as linearity. Therefore, we adopt a function approximation setting under realizability assumptions. We assume that valid causal bounds $[l(a, w), h(a, w)]$ have been obtained using algorithms presented in Section 3.

4.3.1 Function approximation

A practical approach to mitigate dependence on $|\mathcal{W}|$ is to use function approximation methods. We assume the agent has access to a class of reward functions $\mathcal{F} \subset \mathcal{A} \times \mathcal{W} \rightarrow [0, 1]$ (e.g., linear functions) that characterizes the mean reward distribution for a given context-action pair. We impose the following assumption on the realizability of the reward function $\mu_{a,w} = \mathbb{E}[Y | \text{do}(A = a), w]$ within this functional class.

Assumption 4.1 *There exists a function $f^* \in \mathcal{F}$ such that $f^*(a, w) = \mu_{a,w}$, for all $(a, w) \in \mathcal{A} \times \mathcal{W}$.*

This assumption is standard in the contextual bandit literature (Foster and Rakhlin 2020, Foster et al. 2020, Simchi-Levi and Xu 2022). Let $\pi_f(w) = \operatorname{argmax}_{a \in \mathcal{A}} f(a, w)$ denote the policy induced by the regression function $f \in \mathcal{F}$. The set of all induced policies is denoted by $\Pi = \{\pi_f \mid f \in \mathcal{F}\}$, which forms the policy space. The objective of the agent is to achieve low regret with respect to the optimal policy π_{f^*} , and the cumulative regret in (2) reduces to:

$$\operatorname{Reg}(T) = \sum_{t=1}^T \mathbb{E}[f^*(\pi_{f^*}(w_t), w_t) - f^*(a_t, w_t) | w_t]. \quad (16)$$

In the scenario where the agent can observe both contexts W and U during online learning, we modify the realizability assumption as follows to incorporate the influence of context U . Recall that $\mu_{a,w,u} = \mathbb{E}[Y | \text{do}(A = a), w, u]$.

Assumption 4.2 *There exists a function $f^* \in \mathcal{F}$ such that $f^*(a, w, u) = \mu_{a,w,u}$ for all (a, w, u) .*

With a slight abuse of notation, we continue to denote the function space and policy space as \mathcal{F} and Π , respectively. The cumulative regret in (3) can be rewritten as:

$$\operatorname{Reg}(T) = \sum_{t=1}^T f^*(\pi_{f^*}(w_t, u_t), w_t, u_t) - f^*(a_t, w_t, u_t). \quad (17)$$

4.3.2 Transfer learning with function approximation

In the function approximation setting, causal bounds can help refine the set of plausible reward functions, excluding any that fall outside the estimated range. This restricted set of functions is defined as

$$\mathcal{F}^* = \{f \in \mathcal{F} \mid l(a, w) \leq f(a, w) \leq h(a, w)\}.$$

Furthermore, the candidate action set for context w can also be refined using causal bounds:

$$\mathcal{A}^*(w) = \left\{ a \in \mathcal{A} \mid a = \operatorname{argmax}_{i \in \mathcal{A}} f(i, w) \text{ for some } f \text{ in } \mathcal{F}^* \right\}.$$

We propose Algorithm 6 to integrate causal bounds and function approximation in transfer learning for contextual bandits, using the inverse gap weighting (IGW) technique (Agarwal et al. 2012, Foster et al. 2018, 2020, Simchi-Levi and Xu 2022). Unlike prior IGW approaches, which use a fixed action set size $|\mathcal{A}|$ and a non-adaptive learning rate γ (Foster et al. 2018, Simchi-Levi and Xu

2022), our algorithm has three key distinctions. First, we apply the IGW scheme only to functions and actions that remain active based on causal bounds, focusing exploration on promising areas. Second, our learning rate γ_t adapts to each context, capturing the effect of causal bounds on the action set and improving efficiency in online learning. Third, unlike (Foster et al. 2020), our regret rate in T achieves $\mathcal{O}(\sqrt{T \log(\delta^{-1} \log T)})$, improving upon the standard $\mathcal{O}(\sqrt{T \log(\delta^{-1} T^2)} \log T)$. By eliminating suboptimal functions using causal bounds rather than data-driven confidence bounds on the policy space, we effectively avoid the extra $\log T$ factor.

Algorithm 6 Transfer learning for contextual bandit with function approximation

Input: time horizon T , function space \mathcal{F} , confidence parameter δ , tuning parameters η , and causal bounds $[l(a, w), h(a, w)]$

- 1: Eliminate function space \mathcal{F} and obtain \mathcal{F}^* via causal bound
- 2: Set epoch schedule $\{\tau_m = 2^m, \forall m \in \mathbb{N}\}$
- 3: **for** epoch $m = 1, 2, \dots, \lceil \log_2 T \rceil$ **do**
- 4: Compute the least square estimation $\hat{f}_m = \operatorname{argmin}_{f \in \mathcal{F}^*} \sum_{t=1}^{\tau_m-1} (f(a_t, w_t) - y_t)^2$
- 5: **for** round $t = \tau_{m-1} + 1, \dots, \tau_m$ **do**
- 6: Observe the context w_t
- 7: Compute the best action candidate set $\mathcal{A}^*(w_t)$
- 8: Compute $\gamma_t = \sqrt{\frac{\eta |\mathcal{A}^*(w_t)|^{\tau_{m-1}}}{\log(2\delta^{-1} |\mathcal{F}^*| \log T)}}$ (for the first epoch, $\gamma_1 = 1$)
- 9: Compute $\hat{f}_m(a, w_t)$ for each action $a \in \mathcal{A}^*(w_t)$ and the following probabilities

$$p_t(a) = \begin{cases} 0, & \text{for all } a \in \mathcal{A} - \mathcal{A}^*(w_t), \\ \frac{1}{|\mathcal{A}^*(w_t)| + \gamma_t (\hat{f}_m(\hat{a}_t, w_t) - \hat{f}_m(a, w_t))}, & \text{for all } a \in \mathcal{A}^*(w_t) - \{\hat{a}_t\} \\ 1 - \sum_{a \neq \hat{a}_t} p_t(a), & \text{for } a = \hat{a}_t, \end{cases}$$

where $\hat{a}_t = \max_{a \in \mathcal{A}} \hat{f}_m(a, w_t)$.

- 10: Sample $a_t \sim p_t(\cdot)$, take action a_t , and observe a reward y_t
-

In Algorithm 6, calculating \mathcal{F}^* and $\mathcal{A}^*(w)$ can be computationally intensive. A straightforward approach has a time complexity of $\mathcal{O}(|\mathcal{F}|)$, which becomes inefficient for large or infinite $|\mathcal{F}|$. To address this, we compute \mathcal{F}^* implicitly via clipping, using $\min\{\max\{\hat{f}_m(a, w), l(a, w)\}, h(a, w)\}$ as the estimator at each epoch m . As the estimated function \hat{f}_m converges to the true reward function f^* , which lies within the causal bounds, the effect of the bounds diminishes over time. To compute $\mathcal{A}^*(w)$, we refer to Section 4 of (Foster et al. 2020), which outlines a systematic approach to approximate $\mathcal{A}^*(w)$ with a specified accuracy.

An alternative approach to implementing Algorithm 6 is to use expert knowledge $F(a, y, w)$ to compute $\mathbb{E}_W[|\mathcal{A}^*(W)|]$, the expected size of the optimal action set over the context distribution. Using this expectation, we can set $\gamma_t = \sqrt{\frac{\eta \mathbb{E}_W[|\mathcal{A}^*(W)|]^{\tau_{m-1}}}{\log(2\delta^{-1} |\mathcal{F}^*| \log T)}}$, allowing γ_t to remain constant within each epoch. Our proof remains valid with this choice, and the regret bound aligns with the one presented in Theorem 4.5. Intuitively, $|\mathcal{A}(w_t)|$ represents a sample drawn from an induced distribution with mean $\mathbb{E}_W[|\mathcal{A}^*(W)|]$, ensuring that, on average, the regrets of both methods are of the same order.

Theorem 4.5 Consider a contextual bandit problem with $|\mathcal{A}| < \infty$ and $|\mathcal{F}| < \infty$ under **Assumption 4.1**. Assume that the agent has access to the function space \mathcal{F} . With probability at least $1 - \delta$, the expected regret $\mathbb{E}[\text{Reg}(T)]$ of Algorithm 6 is upper bounded by

$$\mathcal{O}\left(\sqrt{\mathbb{E}_W[\mathcal{A}^*(W)]T \log(\delta^{-1}|\mathcal{F}^*| \log T)}\right).$$

As noted by Foster et al. (2020), gap-dependent regret bounds are generally not feasible for contextual bandits, so our focus remains on minimax regret. Previous works, including Liu et al. (2021), Zhang and Bareinboim (2021), have explored transfer learning within general contextual bandits. However, the approach in Zhang and Bareinboim (2021) relies on instrumental variables, resulting in regret bounds that scale with $\sqrt{|\Pi|}$ instead of the more preferable $\sqrt{\log |\Pi|}$. Additionally, identifying instrumental variables remains an open problem in the field. Moreover, (Zhang and Bareinboim 2021) treats each basis policy as an independent arm in bandit settings, a methodology that may overlook the interdependence among policies. In practice, similar policies can provide mutual information. For example, exploring the optimal policy can yield insights into the second-best policy, as these two are likely to differ only in less significant contexts. This understanding explains why their regret scales with $\sqrt{|\Pi|}$ (as $|\Pi| = |\mathcal{F}|$) rather than the more efficient $\sqrt{\log |\Pi|}$.

We now demonstrate that the upper bound in Theorem 4.5 aligns with the minimax lower bound for transfer learning. Define the set of contextual bandit instances with prior knowledge $l(a, w)$ and $h(a, w)$ as

$$\mathfrak{M} = \{\text{contextual bandit instances with } l(a, w) \leq f^*(a, w) \leq h(a, w), \forall (a, w) \in \mathcal{A} \times \mathcal{W}\}.$$

Theorem 4.6 Consider a contextual bandit problem with $|\mathcal{A}| < \infty$ and $|\mathcal{F}| < \infty$ under **Assumption 4.1**. Then for any algorithm A with access to the function space \mathcal{F} , we have

$$\sup_{\mathfrak{M}} \limsup_{T \rightarrow \infty} \frac{\text{Reg}(T)}{\sqrt{T}} \geq \sqrt{\mathbb{E}_W[|\mathcal{A}^*(W)|] \log |\mathcal{F}^*|}.$$

4.4 Task 3: transfer to fully observable contextual bandit

Our approach to Task 3 follows a similar structure to those for Task 1 and Task 2, with modifications to incorporate the additional observability of U . For Task 3, the causal effect in FOCB is estimated as follows:

$$\hat{\mathbb{E}}_{\mathcal{M}}[Y | \text{do}(A = a), w, u] = \sum_j \frac{y_j \theta_l x_{ijkl}}{\sum_{j'} x_{ij'kl}}. \quad (18)$$

With the same optimization framework as (4), but set (18) as the objective function, we can estimate bounds on the causal effect $\mathbb{E}[Y | \text{do}(A = a), w, u]$ by sampling valid causal models using Algorithm 1.

With the causal bounds available, we can filter out functions that cannot represent the true reward function. Specifically, we define the set of feasible reward functions as:

$$\mathcal{F}^* = \{f \in \mathcal{F} | l(a, w, u) \leq f(a, w, u) \leq h(a, w, u)\}.$$

This allows us to redefine the candidate set of optimal arms based on \mathcal{F}^* :

$$\mathcal{A}^*(w, u) = \{a \in \mathcal{A} \mid a = \underset{i \in \mathcal{A}}{\operatorname{argmax}} f(i, w, u) \text{ for some } f \text{ in } \mathcal{F}^*\}.$$

Finally, we apply the adaptive inverse gap weighting method from Algorithm 6 to select actions, yielding the following regret upper bounds. The complete algorithm is presented in Algorithm 9.

Theorem 4.7 *Consider a contextual bandit problem with $|\mathcal{A}| < \infty$ and $|\mathcal{F}| < \infty$ under **Assumption 4.2**. Assume that the agent has access to the function space \mathcal{F} . With probability at least $1 - \delta$, the expected regret $\mathbb{E}[\operatorname{Reg}(T)]$ of Algorithm 9 is upper bounded by*

$$\mathcal{O}\left(\sqrt{\mathbb{E}_{W,U}[\mathcal{A}^*(W,U)]T \log(\delta^{-1}|\mathcal{F}^*| \log T)}\right).$$

4.5 Summary of our results.

Table 4 provides a summary of our theoretical results alongside classical benchmarks. The table illustrates how integrating causal bounds effectively reduces the regret rate by utilizing additional information about the action set size and the function space size. We also discuss some implementation details in Appendix A.

		Classical results	Our results
MAB	Gap-dependent UB	$\sum_{a \in \mathcal{A}, \Delta_a > 0} \frac{\log T}{\Delta_a}$	$\sum_{a \in \widetilde{\mathcal{A}}^*, \Delta_a > 0} \frac{\log T}{\Delta_a}$
	Minimax UB	$\sqrt{ \mathcal{A} T \log T}$	$\sqrt{ \widetilde{\mathcal{A}}^* T \log T}$
	Minimax LB	$\Omega\left(\sqrt{ \mathcal{A} T}\right)$	$\Omega\left(\sqrt{ \widetilde{\mathcal{A}}^* T}\right)$
	Note	$\widetilde{\mathcal{A}}^* := \{a \in \mathcal{A} \mid h(a) \geq \mu^*\} \subset \mathcal{A}$	
CB with finite contexts	Gap-dependent UB	$\sum_{w \in \mathcal{W}} \sum_{a \in \mathcal{A}, \Delta_{w,a} > 0} \frac{\log T}{\Delta_{w,a}}$	$\sum_{w \in \mathcal{W}} \sum_{a \in \widetilde{\mathcal{A}}^*(w), \Delta_{w,a} > 0} \frac{\log T}{\Delta_{w,a}}$
	Minimax UB	$\sqrt{ \mathcal{W} \mathcal{A} T \log T}$	$\sum_{w \in \mathcal{W}} \sqrt{ \widetilde{\mathcal{A}}^*(w) \mathbb{P}(W=w)T \log T}$
	Minimax LB	$\Omega\left(\sqrt{ \mathcal{W} \mathcal{A} T}\right)$	$\Omega\left(\sum_{w \in \mathcal{W}} \sqrt{ \widetilde{\mathcal{A}}^*(w) \mathbb{P}(W=w)T}\right)$
	Note	$\sum_{w \in \mathcal{W}} \sqrt{ \widetilde{\mathcal{A}}^*(w) \mathbb{P}(W=w)} \leq \sqrt{\sum_{w \in \mathcal{W}} \mathcal{A}^*(w) } \leq \sqrt{ \mathcal{W} \mathcal{A} }$	
CB with fuciton approx.	Gap-dependent UB	Not applicable	Not applicable
	Minimax UB	$\sqrt{ \mathcal{A} T \log(\delta^{-1} \mathcal{F} \log T)}$	$\sqrt{\mathbb{E}_W[\mathcal{A}^*(W)]T \log(\delta^{-1} \mathcal{F}^* \log T)}$
	Minimax LB	$\Omega\left(\sqrt{ \mathcal{A} T \log(\mathcal{F})}\right)$	$\Omega\left(\sqrt{\mathbb{E}_W[\mathcal{A}^*(W)]T \log(\mathcal{F}^*)}\right)$
	Note	$\mathcal{F}^* \subset \mathcal{F}$ and $\mathcal{A}^*(w) \subset \mathcal{A}$ for each $w \in \mathcal{W}$	

Table 4: Comparison of classical complexity bounds with our approach. Absolute constants are omitted for clarity. The results for contextual bandit with fuciton approximation is stated for Task 2. For Task 3, one can replace $\mathbb{E}_W[|\mathcal{A}^*(W)|]$ with $\mathbb{E}_{W,U}[\mathcal{A}^*(W,U)]$.

5 Application to Offline Dynamic Pricing

Our causal bounds framework extends seamlessly to a variety of causal graph structures beyond the one depicted in Figure 1, accommodating a wide range of observational distributions and target causal effects.

To illustrate its practical applicability, we consider the offline pricing policy learning problem with censored demand. In this setting, the offline dataset records observed prices P , inventory levels I , and sales S , while the true demand D is unobservable and censored by inventory constraints. In (Tang et al. 2022), the authors propose using an indicator variable to represent the censoring event, presuming that this indicator is observable in the offline data. While this assumption simplifies the identification of the target causal effect, it is quite restrictive and may not hold in many real-world applications, where such indicators are not recorded. We do not require the availability of such indicators.

Our method can be implemented in a streamlined manner to address this problem, as follows:

Step 1: Identify the causal relationships. The first step is to identify the causal relationships among the observed random variables based on the data generation process. Inventory influences price, as pricing decisions are typically adjusted based on observed inventory levels. Inventory also affects sales, as it constrains the fulfillment of demand. Price indirectly influences sales through its impact on the true (but unobserved) demand. This causal structure is depicted in Figure 2.

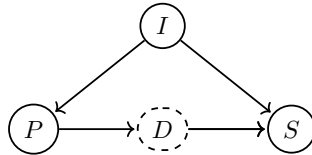


Fig. 2: The causal diagram for offline pricing policy learning with censored demand. Here, P , D , I , and S represent price, demand, inventory, and sales, respectively.

Step 2: Specify the observational distributions and the target causal effect. In practice, the joint distribution $F(p, i, s)$ can be directly estimated from the offline dataset, as all variables are observable. Moreover, the causal relationship among I , D and S is often known a priori, allowing us to assume that the conditional distribution $F(s|d, i)$ is given a priori.

The central goal of offline pricing policy learning is to estimate $\mathbb{E}[D|\text{do}(P = p)]$ using the observational distribution $F(p, i, s)$ and the prior knowledge $F(s|d, i)$. By do-calculus, we can simplify the causal effect $\mathbb{E}[D|\text{do}(P = p)]$ to the conditional expectation $\mathbb{E}[D|p]$ since the backdoor path between P and D is blocked by the variable S , as depicted in Figure 2.

Step 3: Formulate the causal bound optimization problem. Optimizing over all possible causal models compatible with the observational distributions, we obtain the causal bounds for the causal effect $\mathbb{E}[D|p]$:

$$\begin{aligned} & \sup / \inf \mathbb{E}_{\mathcal{M}}[D|p], \\ & \text{s.t. } F_{\mathcal{M}}(p, i, s) = F(p, i, s), \quad F_{\mathcal{M}}(s|d, i) = F(s|d, i). \end{aligned} \tag{19}$$

Our framework provides an efficient Monte Carlo sampling method for generating compatible causal

models, ensuring estimates that converge to valid and tight causal bounds, even in the presence of data censoring.

Building on these causal bounds, we can incorporate pessimistic (Jin et al. 2021) or opportunistic (Stoye 2012) strategies to truncate the confidence bounds. Following the approach in (Bian et al. 2024), finite-sample regret guarantees can be rigorously analyzed for both strategies.

6 Numerical Experiments

Causal bounds.

We compare our proposed Algorithm 2 with the nonlinear optimization method proposed by Li and Pearl (2022) when all variables are binary. Specifically, we randomly generate joint distributions $\mathbb{P}(A, Y, W)$, as shown in Table 5, and set $\mathbb{P}(U = 1) = 0.1$.

(A, Y, W)	(0, 0, 0)	(0, 0, 1)	(0, 1, 0)	(0, 1, 1)	(1, 0, 0)	(1, 0, 1)	(1, 1, 0)	(1, 1, 1)
$\mathbb{P}(a, y, w)$	0.2328	0.1784	0.1351	0.1467	0.0304	0.1183	0.0149	0.1433

Table 5: Observational distribution $\mathbb{P}(A, Y, W)$ for PO CB.

We implemented Algorithm 2 with a batch size of 20000, and set error term $\epsilon = 0$, following Li and Pearl (2022)’s assumption that the given distributions are accurate. The results are presented in Table 6. Our method produces tighter bounds than those obtained by Li and Pearl (2022), as evidenced by the narrower ranges of the estimated causal effects. Additionally, we observed that solving the nonlinear optimization problem is quite unstable and often leads to local optima. To obtain global solutions, we repeated the nonlinear optimization with randomly initialized starting points.

causal effect	Li and Pearl (2022)	Algorithm 2
$\mathbb{E}[Y \text{do}(A = 0)]$	[0.283, 0.505]	[0.352, 0.471]
$\mathbb{E}[Y \text{do}(A = 1)]$	[0.240, 0.807]	[0.265, 0.768]

Table 6: Comparison of causal bounds obtained by Algorithm 2 and Li and Pearl (2022) for PO CB.

Estimation error.

In this numerical experiment, we assess the convergence properties of our proposed method under estimation errors. We utilize the `scipy.optimize.minimize` function from the SciPy library for optimization. The error term ϵ is initialized at 0.1 and applied equally to all probability estimators. As ϵ is gradually reduced towards zero, the optimal values of the optimization problem with error terms steadily converge to those of the original problem, as shown in Figure 3. This observation demonstrates the convergence behavior of our method.

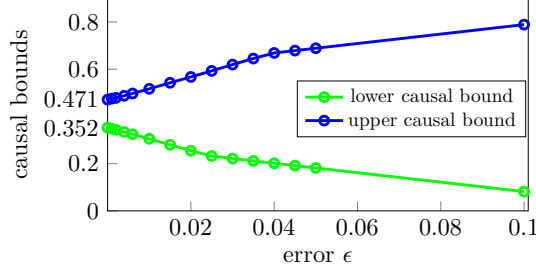


Fig. 3: Estimation for causal bounds $\mathbb{E}[Y|\text{do}(A = 0)]$ with estimation errors of different levels.

Transfer learning in MAB.

We compare our proposed transfer learning algorithm (Algorithm 3) with standard multi-armed bandit (MAB) algorithms that do not utilize causal bounds. We also include a UCB- algorithm that naively transfer knowledge by calculating the conditional expectation $\mathbb{E}[Y|a, w]$ as a surrogate for the true the causal effect $\mathbb{E}[Y|\text{do}(A = a), w]$.

Our simulations involve 5-armed Bernoulli bandits with success probabilities of 0.1, 0.2, 0.3, 0.6, 0.8. The experiments consist of $T = 10^5$ trials, averaged over 50 repetitions. For each task, we collect 1000 samples generated by a source agent to compute the empirical joint distribution.

The estimated causal bounds without knowledge of $F(u)$ (denoted as CUCB in Figure 3) are $h(a) = 0.9, 0.35, 0.92, 0.96, 0.92$, and $l(a) = 0, 0.08, 0.1, 0.3, 0.4$ following the method proposed by Zhang and Bareinboim (2017). In contrast, our method, which incorporates knowledge of $F(u)$ yields significantly tighter bounds: $h(a) = 0.2, 0.25, 0.77, 0.7, 0.9$, and $l(a) = 0.01, 0.08, 0.19, 0.38, 0.71$. This substantial narrowing highlights the advantage of our approach in providing more precise estimates of causal effects.

The regret curves, as shown in Figure 4, reveal key insights. The regret of UCB- initially grows linearly before transitioning to a sublinear trend, highlighting the negative transfer effect where the agent spends many trials mitigating the impact of incorrect knowledge. Additionally, we observe that causal bounds can improve regret performance even when no arms are eliminated, as evidenced by the comparison between CUCB and UCB. Most notably, our proposed algorithm achieves significantly faster convergence rates by leveraging tighter causal bounds to effectively eliminate suboptimal arms. These findings validate our approach and demonstrate that offline data can be effectively used to improve the target agent’s performance, even in situations where causal identifiability is not achievable.

Transfer learning in contextual bandits.

We generate function space $\mathcal{F} = (w - w_0)^\top (a - a_0)$ of size 50 by sampling parameters w_0 and a_0 in \mathbb{R}^d from $\mathcal{N}(0, 0.1)$, where $d = 10$. A true reward function f^* is randomly selected from the first 5 functions in \mathcal{F} . The reward is then generated as

$$Y = f^*(W, A) + \mathcal{N}(0, 0.1),$$

where the context W is drawn i.i.d. from a standard normal distribution, and A is the selected action. The action set \mathcal{A} is initialized uniformly at random from $[-1, 1]^d$ with a size of 10. Each

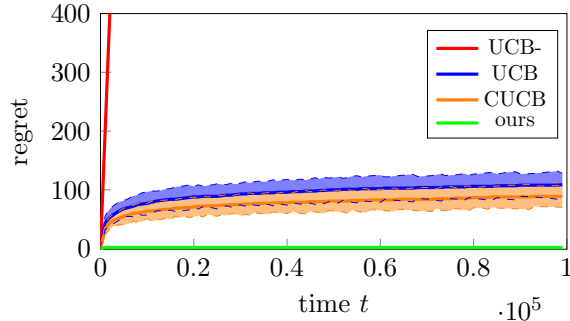


Fig. 4: Comparison of classical and causally enhanced algorithms. The solid curves represent the average cumulative regret over time for each algorithm. The top and bottom dashed curves correspond to one standard deviation added to and subtracted from the mean cumulative regret.

experiment is repeated 50 times to smooth the regret curves.

We compare the performance of our algorithm with FALCON (Simchi-Levi and Xu 2022), a well-known implementation of IGW. The numerical results in Figure 5 demonstrate that our algorithm significantly outperforms FALCON, even without explicitly removing infeasible functions. In the experiments, the average size of the action subset $\mathcal{A}(w)$ is 3.254, highlighting the substantial performance gains achieved by reducing the size of the action space. Additionally, our algorithm excels with homogeneous functions, which often attain their maximum values at the same points. In such scenarios, adaptively eliminating suboptimal actions proves to be a highly effective strategy for minimizing regrets.

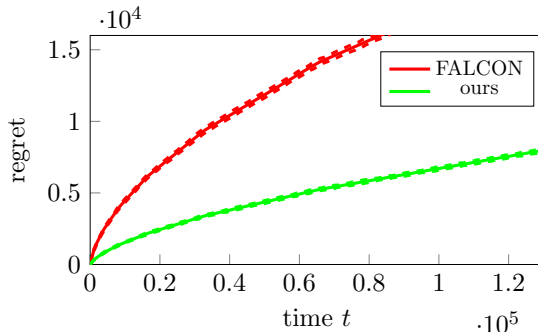


Fig. 5: Comparison of classical and causally enhanced algorithms in function approximation settings. The solid curves represent the average cumulative regret over time for each algorithm. The top and bottom dashed curves correspond to one standard deviation added to and subtracted from the mean cumulative regret.

7 Conclusions

In this paper, we explored a practical transfer learning setting where incomplete offline datasets hinder direct reward estimation. We demonstrated that naive approaches in such scenarios can result in negative transfer, emphasizing the need to focus on transferring causal effects. Given the challenges posed by the non-identifiability of causal effects in the presence of unobserved confounders, we instead derived tight causal bounds as a more robust alternative.

We proposed a series of optimization problems to compute these causal bounds. To ensure computational feasibility, we introduced a method based on solving a sequence of linear programs to generate valid causal models. Our framework is designed to accommodate both estimation and approximation errors effectively. Moreover, we showed that incorporating optimization procedures enhances convergence rates. In transfer learning tasks, leveraging causal bounds allowed us to eliminate suboptimal actions, achieving consistent improvements over classical bandit algorithms and significantly accelerating convergence.

There are several future research directions worth exploring. While the approximation error is zero for discrete random variables, it remains an open question under what conditions on general random variables and discretization methods the solutions to the discretized optimization converge to those of the original continuous problem. Our numerical results indicate convergence for specific discrete distributions, and we hypothesize that this behavior may be tied to the sensitivity of the underlying nonlinear optimization problem. Additionally, an extension of our IGW-based algorithm to settings with continuous action spaces would be valuable. IGW has shown promise in such contexts and demonstrated practical advantages in large action spaces. This extension could involve exploring complexity measures from machine learning to guide the design of efficient algorithms for continuous action settings.

References

- Agarwal, A., Dudík, M., Kale, S., Langford, J., and Schapire, R. (2012). Contextual bandit learning with predictable rewards. In *Artificial Intelligence and Statistics*, pages 19–26. PMLR.
- Bareinboim, E., Forney, A., and Pearl, J. (2015). Bandits with unobserved confounders: A causal approach. *Advances in Neural Information Processing Systems*, 28.
- Bian, Z., Qi, Z., Shi, C., and Wang, L. (2024). A tale of two cities: Pessimism and opportunism in offline dynamic pricing. *arXiv preprint arXiv:2411.08126*.
- Bilaj, S., Dhouib, S., and Maghsudi, S. (2023). Hypothesis transfer in bandits by weighted models. In *Machine Learning and Knowledge Discovery in Databases: European Conference, ECML PKDD 2022, Grenoble, France, September 19–23, 2022, Proceedings, Part IV*, pages 284–299. Springer.
- Bu, J., Simchi-Levi, D., and Xu, Y. (2020). Online pricing with offline data: Phase transition and inverse square law. In *International Conference on Machine Learning*, pages 1202–1210. PMLR.
- Buckman, J., Gelada, C., and Bellemare, M. G. (2020). The importance of pessimism in fixed-dataset policy optimization. *arXiv preprint arXiv:2009.06799*.
- Cai, C., Cai, T. T., and Li, H. (2024). Transfer learning for contextual multi-armed bandits. *The Annals of Statistics*, 52(1):207–232.
- Chen, S., Wang, Y., Wang, Z., and Yang, Z. (2023). A unified framework of policy learning for contextual bandit with confounding bias and missing observations. *arXiv preprint arXiv:2303.11187*.
- Chu, W., Li, L., Reyzin, L., and Schapire, R. (2011). Contextual bandits with linear payoff functions. In *Proceedings of the Fourteenth International Conference on Artificial Intelligence and Statistics*, pages 208–214. JMLR Workshop and Conference Proceedings.
- Dann, C., Marinov, T. V., Mohri, M., and Zimmert, J. (2021). Beyond value-function gaps: Improved instance-dependent regret bounds for episodic reinforcement learning. *Advances in Neural Information Processing Systems*, 34:1–12.
- Duarte, G., Finkelstein, N., Knox, D., Mummolo, J., and Shpitser, I. (2024). An automated approach to causal inference in discrete settings. *Journal of the American Statistical Association*, 119(547):1778–1793.
- Eberhardt, F., Kaynar, N., and Siddiq, A. (2024). Discovering causal models with optimization: Confounders, cycles, and instrument validity. *Management Science*.
- Fan, K. (1953). Minimax theorems. *Proceedings of the National Academy of Sciences of the United States of America*, 39(1):42.
- Foster, D., Agarwal, A., Dudík, M., Luo, H., and Schapire, R. (2018). Practical contextual bandits with regression oracles. In *International Conference on Machine Learning*, pages 1539–1548. PMLR.
- Foster, D. and Rakhlin, A. (2020). Beyond UCB: Optimal and efficient contextual bandits with regression oracles. In *International Conference on Machine Learning*, pages 3199–3210. PMLR.
- Foster, D. J., Rakhlin, A., Simchi-Levi, D., and Xu, Y. (2020). Instance-dependent complexity of contextual bandits and reinforcement learning: A disagreement-based perspective. *arXiv preprint arXiv:2010.03104*.
- Gong, X. and Zhang, J. (2023). Achieving near-optimal regrets in confounded contextual bandits. In *Proceedings of the 2023 International Conference on Autonomous Agents and Multiagent Systems*, pages 2643–2645.
- Guo, H., Cai, Q., Zhang, Y., Yang, Z., and Wang, Z. (2022). Provably efficient offline reinforcement learning for partially observable Markov decision processes. In *International Conference on Machine Learning*, pages 8016–8038. PMLR.

- Islam, M. S., Morshed, M. S., and Noor-E-Alam, M. (2022). A computational framework for solving nonlinear binary optimization problems in robust causal inference. *INFORMS Journal on Computing*, 34(6):3023–3041.
- Jin, C., Yang, Z., Wang, Z., and Jordan, M. I. (2020). Provably efficient reinforcement learning with linear function approximation. In *Conference on learning theory*, pages 2137–2143. PMLR.
- Jin, Y., Yang, Z., and Wang, Z. (2021). Is pessimism provably efficient for offline RL? In *International Conference on Machine Learning*, pages 5084–5096. PMLR.
- Kallus, N. (2018). Instrument-armed bandits. In *Algorithmic Learning Theory*, pages 529–546. PMLR.
- Lattimore, F., Lattimore, T., and Reid, M. D. (2016). Causal bandits: Learning good interventions via causal inference. *Advances in Neural Information Processing Systems*, 29.
- Lattimore, T. and Szepesvári, C. (2020). *Bandit algorithms*. Cambridge University Press.
- Lazaric, A., Brunskill, E., et al. (2013). Sequential transfer in multi-armed bandit with finite set of models. *Advances in Neural Information Processing Systems*, 26.
- Li, A., Jiang, S., Sun, Y., and Pearl, J. (2022). Learning probabilities of causation from finite population data. *arXiv preprint arXiv:2210.08453*.
- Li, A., Mueller, S., and Pearl, J. (2023). Epsilon-identifiability of causal quantities. *arXiv preprint arXiv:2301.12022*.
- Li, A. and Pearl, J. (2022). Bounds on causal effects and application to high dimensional data. In *Proceedings of the AAAI Conference on Artificial Intelligence*, volume 36, pages 5773–5780.
- Li, A. and Pearl, J. (2024a). Probabilities of causation with nonbinary treatment and effect. In *Proceedings of the AAAI Conference on Artificial Intelligence*, volume 38, pages 20465–20472.
- Li, A. and Pearl, J. (2024b). Unit selection with nonbinary treatment and effect. In *Proceedings of the AAAI Conference on Artificial Intelligence*, volume 38, pages 20473–20480.
- Li, L., Chu, W., Langford, J., and Schapire, R. E. (2010). A contextual-bandit approach to personalized news article recommendation. In *Proceedings of the 19th international conference on World wide web*, pages 661–670.
- Liu, B., Wei, Y., Zhang, Y., Yan, Z., and Yang, Q. (2018). Transferable contextual bandit for cross-domain recommendation. In *Proceedings of the AAAI Conference on Artificial Intelligence*, volume 32.
- Liu, C., Zhang, Y., Shen, Y., and Zavlanos, M. M. (2021). Learning without knowing: Unobserved context in continuous transfer reinforcement learning. In *Learning for Dynamics and Control*, pages 791–802. PMLR.
- Lu, M., Min, Y., Wang, Z., and Yang, Z. (2023). Pessimism in the face of confounders: Provably efficient offline reinforcement learning in partially observable Markov decision processes.
- Nikolaev, A. G., Jacobson, S. H., Cho, W. K. T., Sauppe, J. J., and Sewell, E. C. (2013). Balance optimization subset selection (BOSS): An alternative approach for causal inference with observational data. *Operations Research*, 61(2):398–412.
- Park, H. and Faradonbeh, M. K. S. (2021). Analysis of Thompson sampling for partially observable contextual multi-armed bandits. *IEEE Control Systems Letters*, 6:2150–2155.
- Pearl, J. (2009). Causal inference in statistics: An overview. *Statistics surveys*, 3:96–146.
- Pearl, J. and Mackenzie, D. (2018). *The book of why: the new science of cause and effect*. Basic books.
- Ren, Z., Tian, J., Kang, S., Tang, M., and Tian, J. (2024). Personalized pricing versus showrooming: competition between online and offline retailers. *International Transactions in Operational Research*, 31(5):3371–3442.
- Rosenstein, M. T., Marx, Z., Kaelbling, L. P., and Dietterich, T. G. (2005). To transfer or not to transfer. In *NIPS 2005 workshop on transfer learning*, volume 898, page 4.

- Shi, C., Uehara, M., Huang, J., and Jiang, N. (2022). A minimax learning approach to off-policy evaluation in confounded partially observable Markov decision processes. In *International Conference on Machine Learning*, pages 20057–20094. PMLR.
- Shridharan, M. and Iyengar, G. (2022). Scalable computation of causal bounds. In *International Conference on Machine Learning*, pages 20125–20140. PMLR.
- Simchi-Levi, D. and Xu, Y. (2022). Bypassing the monster: A faster and simpler optimal algorithm for contextual bandits under realizability. *Mathematics of Operations Research*, 47(3):1904–1931.
- Stoye, J. (2012). Minimax regret treatment choice with covariates or with limited validity of experiments. *Journal of Econometrics*, 166(1):138–156.
- Tang, J., Qi, Z., Fang, E., and Shi, C. (2022). Offline feature-based pricing under censored demand: A causal inference approach. *Available at SSRN 4040305*.
- Tennenholtz, G., Shalit, U., Mannor, S., and Efroni, Y. (2021). Bandits with partially observable confounded data. In *Uncertainty in Artificial Intelligence*, pages 430–439. PMLR.
- Tian, J. and Pearl, J. (2002). A general identification condition for causal effects. In *Eighteenth National Conference on Artificial Intelligence*, pages 567–573, USA. American Association for Artificial Intelligence.
- Uehara, M., Sekhari, A., Lee, J. D., Kallus, N., and Sun, W. (2022). Provably efficient reinforcement learning in partially observable dynamical systems. *Advances in Neural Information Processing Systems*, 35:578–592.
- Wang, L., Yang, Z., and Wang, Z. (2021). Provably efficient causal reinforcement learning with confounded observational data. *Advances in Neural Information Processing Systems*, 34:21164–21175.
- Xu, L., Kanagawa, H., and Gretton, A. (2021). Deep proxy causal learning and its application to confounded bandit policy evaluation. *Advances in Neural Information Processing Systems*, 34.
- Yu, T., Thomas, G., Yu, L., Ermon, S., Zou, J. Y., Levine, S., Finn, C., and Ma, T. (2020). MOPO: Model-based offline policy optimization. *Advances in Neural Information Processing Systems*, 33:14129–14142.
- Zhang, J. and Bareinboim, E. (2017). Transfer learning in multi-armed bandit: a causal approach. In *Proceedings of the 16th Conference on Autonomous Agents and MultiAgent Systems*, pages 1778–1780.
- Zhang, J. and Bareinboim, E. (2021). Bounding causal effects on continuous outcome. In *Proceedings of the AAAI Conference on Artificial Intelligence*, volume 35, pages 12207–12215.
- Zhang, J., Tian, J., and Bareinboim, E. (2022). Partial counterfactual identification from observational and experimental data. In *International Conference on Machine Learning*, pages 26548–26558. PMLR.
- Zhuang, F., Qi, Z., Duan, K., Xi, D., Zhu, Y., Zhu, H., Xiong, H., and He, Q. (2020). A comprehensive survey on transfer learning. *Proceedings of the IEEE*, 109(1):43–76.

A Discussions

Acceleration of sampling.

To accelerate the convergence of Algorithm 2, we incorporate an optimization procedure `OPT` that accepts the objective function to minimize or maximize, the feasible domain \mathcal{D} , and an initial guess \mathbf{x}_0 . The procedure `OPT` seeks a local optimum $\mathbf{x}_{loc} \in \mathcal{D}$ that optimizes the objective function locally. We present the algorithm for general causal effect targets in Algorithm 8. In each iteration of Algorithm 2, we use the sampled value \mathbf{x}^τ as the initial guess \mathbf{x}_0 and input it into `OPT`. The output of `OPT` then serves as an updated estimate of the causal bounds. By leveraging this optimization procedure, we can enhance the convergence results in Proposition 3.1 under the following assumption on `OPT`.

Assumption A.1 *OPT is deterministic and satisfies the following property: For any local optimum \mathbf{x}_{loc} within the feasible domain \mathcal{D} , there exists a $\delta > 0$ such that, for any initial guess $\mathbf{x}_0 \in \mathcal{B}(\mathbf{x}_{loc}, \delta) \cap \mathcal{D}$, the procedure `OPT` will output \mathbf{x}_{loc} .*

Proposition A.1 *Assume that the sampling measure \mathbb{P}_s satisfies $\forall \mathbf{x} \in \mathcal{D}$, and $\forall \delta > 0$,*

$$\mathbb{P}_s(\mathcal{B}(\mathbf{x}, \delta) \cap \mathcal{D}) > 0,$$

*where $\mathcal{B}(\mathbf{x}, \delta)$ is a ball centered at \mathbf{x} with radius δ . Let $l_B(a), h_B(a)$ be the outputs of Algorithm 8 with the target (6) and an optimization procedure `OPT` that satisfies **Assumption A.1**, then $l_B(a)$ and $h_B(a)$ converge almost surely to $l(a)$ and $h(a)$ as $B \rightarrow \infty$, respectively.*

These results suggest that the modified algorithm incorporating `OPT` converges to the optimal solution at a faster rate than the original algorithm. Intuitively, the optimization procedure `OPT` concentrates the sampling probability around the local optima rather than spreading it over the entire feasible domain. Since optimization procedures typically perform effectively in local regions and can guarantee local optimality for sufficiently close initial guesses, our assumption on `OPT` is reasonable and not overly restrictive. Similar convergence results also apply to the causal bounds in (14). For detailed proofs, please refer to Proposition C.2 and Proposition C.3 in the Appendix.

Infinite function classes.

We note that Algorithm 6 and Theorem 4.5 naturally extend to infinite function classes \mathcal{F} . In such cases, the dependence on $\log |\mathcal{F}^*|$ in the algorithm's parameters and regret bounds is replaced by standard learning-theoretic complexity measures, such as metric entropy. Suppose \mathcal{F} is equipped with a maximum norm $\|\cdot\|$. Consider an ϵ -covering \mathcal{F}_ϵ^* of \mathcal{F}^* so that for any reward function f^* , there exists a function $f_\epsilon^* \in \mathcal{F}_\epsilon^*$ such that $\|f_\epsilon^* - f^*\| \leq \epsilon$. Since $|\mathcal{F}_\epsilon^*|$ is finite, we can replace \mathcal{F}^* with \mathcal{F}_ϵ^* without altering any algorithmic procedures. Hence, the regret can be bounded by

$$\text{Reg}(T) \leq 8\sqrt{\mathbb{E}_W[\mathcal{A}(W)]T \log(2\delta^{-1}|\mathcal{F}_\epsilon^*| \log T)} + \epsilon T$$

By setting $\epsilon = \frac{1}{T}$, we obtain a result similar to Theorem 4.5.

Definition A.1 (Fan 1953) Let $(\mathcal{F}, \|\cdot\|)$ be a normed space. A set $\{f_1, \dots, f_N\}$ is an ϵ -covering of \mathcal{F} if, for every $f \in \mathcal{F}$, there exists an i such that $\|f - f_i\| \leq \epsilon$. The covering number $N(\mathcal{F}, \|\cdot\|, \epsilon)$ is defined as the minimal cardinality N over all ϵ -coverings of \mathcal{F} .

It clear that $\text{Reg}(T)$ scales with $\sqrt{\log N(\mathcal{F}^*, \|\cdot\|, \epsilon)}$. Note that $N(\mathcal{F}^*, \|\cdot\|, \epsilon) \leq N(\mathcal{F}, \|\cdot\|, \epsilon)$ since $\mathcal{F}^* \subset \mathcal{F}$. The covering number explicitly shows how causal bounds help improve the algorithm’s performance by reducing the search space.

Let $m = \inf_{w,a} l(w, a)$ and $M = \sup_{w,a} h(w, a)$. These bounds chip away the surface of the unit sphere and scoop out the concentric sphere of radius m . Therefore, the transfer learning algorithm only needs to search within a “spherical shell” of thickness $M - m$ at most.

Implementation details.

Computing \mathcal{F}^* and $\mathcal{A}(w)$ directly can be computationally intensive. A naive approach has a time complexity of $\mathcal{O}(|\mathcal{F}|)$, which becomes inefficient for large or infinite function classes $|\mathcal{F}|$ and infeasible for infinite $|\mathcal{F}|$. To address this, we can implicitly compute \mathcal{F}^* by applying clipping to the estimator $\hat{f}_m(w, a)$ at each epoch m :

$$\hat{f}'_m(w, a) \triangleq \min\{\max\{\hat{f}_m(w, a), l(w, a)\}, h(w, a)\}.$$

This approach ensures that $\hat{f}'_m(w, a)$ remains within the causal bounds $[l(w, a), h(w, a)]$. As $\hat{f}_m(w, a)$ converges to the true reward function f^* , which lies within these bounds, the influence of the clipping diminishes. For computing $\mathcal{A}(w)$, we refer to Section 4 of Foster et al. (2020), which provides a systematic method for determining $\mathcal{A}(w)$ with a specified accuracy.

An alternative approach to implement Algorithm 6 is to estimate $\mathbb{E}_W[|\mathcal{A}(W)|]$ using expert knowledge $F(a, y, w)$. We can then set the learning rate $\gamma_t = \sqrt{\frac{\eta \mathbb{E}_W[|\mathcal{A}(W)|] \tau_{m-1}}{\log(2\delta^{-1}|\mathcal{F}^*| \log T)}}$, ensuring that γ_t remains constant within each epoch. Our proof remains valid with this choice, and the regret bound is the same as in Theorem 4.5. Intuitively, $|\mathcal{A}(w_t)|$ is a sample from a distribution with mean $\mathbb{E}_W[|\mathcal{A}(W)|]$, so on average, the regrets of both methods are of the same order.

B Additional Algorithms

In this section, we extend the sampling method presented in Algorithm 2 to a more general algorithm, Algorithm 7, which samples a random point within a simplex $\mathcal{D} \subset \mathbb{R}^d$ defined by

$$\mathcal{D} \triangleq \{\mathbf{x} \in \mathbb{R}^d : A\mathbf{x} \leq \mathbf{b}, \mathbf{x} \geq \mathbf{0}\}.$$

Without loss of generality, we always assume \mathcal{D} is not empty.

Algorithm 7 A sampling algorithm for the given simplex

Input: A simplex $\mathcal{D} = \{\mathbf{x} : A\mathbf{x} \leq \mathbf{b}, \mathbf{x} \geq \mathbf{0}\}$ and a sampling distribution F_s supported on $[0, 1]$ 1: Solving the following LP to find the bound $[l_1, h_1]$ for x_1

$$\begin{aligned} & \max / \min x_1, \\ & \text{s.t. } A\mathbf{x} \leq \mathbf{b}, \mathbf{x} \geq \mathbf{0}. \end{aligned}$$

2: Sample a value \hat{x}_1 from the truncated F_s supported on $[l_1, h_1]$ 3: **for** $i = 2, \dots, d$ **do**4: Solving the follow LP to find the bound $[l_i, h_i]$ for x_i

$$\begin{aligned} & \max / \min x_1, \\ & \text{s.t. } A\mathbf{x} \leq \mathbf{b}, \mathbf{x} \geq \mathbf{0}, \\ & \quad x_j = \hat{x}_j, j = 1, \dots, i-1. \end{aligned}$$

5: Sample a value \hat{x}_i from the truncated F_s supported on $[l_i, h_i]$ **Output:** The sample $\hat{\mathbf{x}} = (\hat{x}_1, \dots, \hat{x}_d) \in \mathcal{D}$

Algorithm 8 Monte-Carlo estimation for causal bounds with an extra optimization procedure

Input: Sample size B , optimization procedure **OPT**, target causal effect CE 1: **for** $\tau = 1, 2, \dots, B$ **do**2: Call Algorithm 1 to obtain the sampled causal model $\hat{\mathbf{x}}^\tau$ 3: Use the obtained feasible sample $\hat{\mathbf{x}}^\tau$ as the initial guess into **OPT** and obtain samples of causal effects CE_τ through minimization/maximization problems4: Compute $LB = \min_\tau CE_\tau$ and $UB = \max_\tau CE_\tau$ **Output:** $\{LB, UB\}$

Algorithm 9 Transfer learning for contextual bandit with function approximation

Require: time horizon T , function space \mathcal{F} , confidence parameter δ , tuning parameters η , and causal bounds $[l(a, w, u), h(a, w, u)]$

- 1: Eliminate function space \mathcal{F} and obtain \mathcal{F}^* via causal bound
- 2: Set epoch schedule $\{\tau_m = 2^m, \forall m \in \mathbb{N}\}$
- 3: **for** epoch $m = 1, 2, \dots, \lceil \log_2 T \rceil$ **do**
- 4: Compute the least square estimation

$$\hat{f}_m = \underset{f \in \mathcal{F}^*}{\operatorname{argmin}} \sum_{t=1}^{\tau_{m-1}} (f(a_t, w_t, u_t) - y_t)^2$$

- 5: **for** round $t = \tau_{m-1} + 1, \dots, \tau_m$ **do**
- 6: Observe the context w_t, u_t
- 7: Compute the best action candidate set $\mathcal{A}^*(w_t, u_t)$
- 8: Compute $\gamma_t = \sqrt{\frac{\eta |\mathcal{A}^*(w_t, u_t)|^{\tau_{m-1}}}{\log(2\delta^{-1} |\mathcal{F}^*| \log T)}}$ (for the first epoch, $\gamma_1 = 1$)
- 9: Compute $\hat{f}_m(w_t, u_t, a)$ for each action $a \in \mathcal{A}^*(w_t, u_t)$ and the following probabilities

$$p_t(a) = \begin{cases} 0, & \text{for all } a \in \mathcal{A} - \mathcal{A}^*(w_t, u_t), \\ \frac{1}{|\mathcal{A}^*(w_t, u_t)| + \gamma_t (\hat{f}_m(\hat{a}_t, w_t, u_t) - \hat{f}_m(a, w_t, u_t))}, & \text{for all } a \in \mathcal{A}^*(w_t, u_t) - \{\hat{a}_t\} \\ 1 - \sum_{a \neq \hat{a}_t} p_t(a), & \text{for } a = \hat{a}_t, \end{cases}$$

where $\hat{a}_t = \max_{a \in \mathcal{A}} \hat{f}_m(a, w_t, u_t)$.

- 10: Sample $a_t \sim p_t(\cdot)$, take action a_t , and observe a reward y_t
-

C Proofs

C.1 Proof of the mentioned facts

Fact C.1.1 *Given a series of known observational distributions F^1, \dots, F^n , consider the following optimization problem to determine bounds on the causal effect:*

$$\begin{aligned} & \sup / \inf CE(\mathcal{M}), \\ & \text{s.t. } F_{\mathcal{M}}^i = F^i, i = 1, \dots, n, \end{aligned}$$

where $CE(\mathcal{M})$ represents the desired causal effect, and $F_{\mathcal{M}}^i$ denotes the distribution induced by the causal model \mathcal{M} corresponding to the observational distribution F^i . Here, the *sup/inf* is taken with respect to all causal models \mathcal{M} that are compatible with the given observational distributions. A causal effect $CE(\mathcal{M})$ is identifiable if and only if the lower bound (LB) and upper bound (UB) solutions to the optimization problem are equal, i.e., $LB = UB$.

Proof. If $LB = UB$, then for any compatible model \mathcal{M}_1 and \mathcal{M}_2 , we have

$$LB = CE(\mathcal{M}_1) = CE(\mathcal{M}_2) = UB.$$

According the definition of causal identification, the required causal effect $CE(\mathcal{M})$ can be fully identified.

On the contrary, suppose $CE(\mathcal{M})$ is causal identifiable. Then for any compatible model pair \mathcal{M}_1 and \mathcal{M}_2 , we have $CE(\mathcal{M}_1) = CE(\mathcal{M}_2)$. Traveling over all compatible models immediately yields

$$LB = CE(\mathcal{M}_1) = CE(\mathcal{M}_2) = UB.$$

□

Fact C.1.2 *If the estimator $\hat{\theta}_x$ for $\theta_x \in [0, 1]$ has n_x i.i.d. samples, then the variance of $\hat{\theta}_x$ is at most $\frac{1}{4n_x}$.*

Proof. Since $\theta_x^2 \leq \theta_x$, then

$$\text{Var}(\theta_x) = \mathbb{E}[\theta_x^2] - (\mathbb{E}[\theta_x])^2 \leq \mathbb{E}[\theta_x] - (\mathbb{E}[\theta_x])^2 \leq \frac{1}{4}.$$

Hence, we have

$$\text{Var}(\hat{\theta}_x) = \frac{1}{n_x} \text{Var}(\theta_x) \leq \frac{1}{4n_x}.$$

□

C.2 Optimization problem for general distributions

Theorem C.1 *Given a causal diagram \mathcal{G} and a distribution compatible with \mathcal{G} , let (W, U) be a set of variables satisfying the back-door criterion in \mathcal{G} relative to an ordered pair (A, Y) , where (W, U) is partially observable, i.e., only probabilities $\hat{F}(a, y, w)$ and $\hat{F}(u)$ with the maximum estimation error ϵ are observed, then the causal effects of A on Y are bounded as follows:*

$$l(a_0) \leq \mathbb{E}[Y | \text{do}(A = a_0)] \leq h(a_0),$$

where $l(a_0)$ and $h(a_0)$ are solutions to the following functional optimization problem for any given a_0

$$\begin{aligned} l(a_0) &= \inf \int_{w \in \mathcal{W}, u \in \mathcal{U}} \int_{y \in \mathcal{Y}} y dF(y | a_0, w, u) dF(w, u) \\ h(a_0) &= \sup \int_{w \in \mathcal{W}, u \in \mathcal{U}} \int_{y \in \mathcal{Y}} y dF(y | a_0, w, u) dF(w, u) \\ \text{s.t.} \quad &\int_{u \in \mathcal{U}} dF(a, y, w, u) = F(a, y, w), \forall (a, y, w) \in \mathcal{A} \times \mathcal{Y} \times \mathcal{W} \\ &\int_{a \in \mathcal{A}, y \in \mathcal{Y}, w \in \mathcal{W}} dF(a, y, w, u) = F(u), \forall u \in \mathcal{U} \\ &\int_{y \in \mathcal{Y}} dF(a, y, w, u) = F(a, w, u), \forall (a, w, u) \in \mathcal{A} \times \mathcal{W} \times \mathcal{U} \\ &\int_{a \in \mathcal{A}} dF(a, w, u) du = F(w, u), \forall (w, u) \in \mathcal{W} \times \mathcal{U} \\ &F(y | a, w, u) F(a, w, u) = F(a, y, w, u), \forall (a, y, w, u) \in \mathcal{A} \times \mathcal{Y} \times \mathcal{W} \times \mathcal{U} \\ &|F(a, y, w) - \hat{F}(a, y, w)| \leq \epsilon, \forall (a, y, w) \in \mathcal{A} \times \mathcal{Y} \times \mathcal{W} \\ &|F(u) - \hat{F}(u)| \leq \epsilon, \forall u \in \mathcal{U}. \end{aligned}$$

Here the *inf/sup* is taken with respect to all unknown cumulative distribution functions $F(a, y, w, u)$, $F(a, w, u)$, $F(y|a, w, u)$, $F(w, u)$, $F(a, y, w)$ and $F(u)$.

The functional optimization problem presented in (4) provides tight lower and upper bounds on the average causal effect $l(a)$ and $h(a)$, respectively, for any given $a \in \mathcal{A}$. This optimization problem can be applied to both parametric and non-parametric cases. We first consider the accurate observational distribution, and further discuss how to incorporate the influence of estimation errors.

Proof. Since W and U satisfies the back-door criterion, we can condition on W, U to identify the causal effect $\mathbb{E}[Y|\text{do}(A = a_0)]$. We have

$$\begin{aligned}\mathbb{E}[Y|\text{do}(A = a_0)] &= \int_{w \in \mathcal{W}, u \in \mathcal{U}} \mathbb{E}[Y|\text{do}(A = a_0), w, u] dF(w, u) \\ &= \int_{w \in \mathcal{W}, u \in \mathcal{U}} \mathbb{E}[Y|a_0, w, u] dF(w, u) \\ &= \int_{w \in \mathcal{W}, u \in \mathcal{U}} \int_{y \in \mathcal{Y}} y dF(y|a_0, w, u) dF(w, u).\end{aligned}$$

The equalities come from the normalization properties of distribution functions. The inequalities come from the estimation error. \square

For continuous random variables, we can discrete distributions as the same way in Section 3.3. During discretization, equality constraints in Theorem C.1 are automatically satisfied in the sense of integration.

For the first constraint, we integrate over $\mathcal{A}_i \times \mathcal{Y}_j \times \mathcal{W}_k$ and have

$$\begin{aligned}\int_{a \in \mathcal{A}_i, y \in \mathcal{Y}_j, w \in \mathcal{W}_k} dF(a, y, w) du &= \int_{a \in \mathcal{A}_i, y \in \mathcal{Y}_j, w \in \mathcal{W}_k, u \in \mathcal{U}} dF(a, y, w, u) du \\ &= \sum_l \int_{a \in \mathcal{A}_i, y \in \mathcal{Y}_j, w \in \mathcal{W}_k, u \in \mathcal{U}} dF(a, y, w, u) du \\ &= \sum_l x_{ijkl}.\end{aligned}$$

For the second equality, we integrate over \mathcal{U}_l and have

$$\begin{aligned}\int_{u \in \mathcal{U}_l} dF(u) du &= \int_{a \in \mathcal{A}, y \in \mathcal{Y}, w \in \mathcal{W}, u \in \mathcal{U}_l} dF(a, y, w, u) du \\ &= \sum_{ijk} \int_{a \in \mathcal{A}_i, y \in \mathcal{Y}_j, w \in \mathcal{W}_k, u \in \mathcal{U}_l} dF(a, y, w, u) du \\ &= \sum_{ijk} x_{ijkl}.\end{aligned}$$

Hence, the second equality constraint holds in the sense of integration.

For the third and the fourth equality constrains, we can do integration over corresponding blocks and check the equality in the same way. The conditional distribution in the fifth equality can be approximated by x_{ijkl} . We now discuss the object in Theorem C.1 after discretization, which is approximately equal to (6).

We use the average values to approximate distributions at certain points. First, we only need to consider the value

$$\int_{y \in \mathcal{Y}_j, w \in \mathcal{W}_k, u \in \mathcal{U}_l} y \frac{dF(a, y, w, u) dF(w, u)}{dF(a, w, u)},$$

as summing over j, k, l can yield the object.

Suppose the given $a \in \mathcal{A}_i$ and let $\text{vol}(\cdot)$ denote the volume of the given block. For the values of distributions in $\mathcal{A}_i \times \mathcal{Y}_j \times \mathcal{W}_k \times \mathcal{U}_l$, we have

$$\begin{aligned} dF(a, y, w, u) &\approx \frac{dad y d w d u}{\text{vol}(\mathcal{A}_i) \text{vol}(\mathcal{Y}_j) \text{vol}(\mathcal{W}_k) \text{vol}(\mathcal{U}_l)} \int_{a \in \mathcal{A}_i, y \in \mathcal{Y}_j, w \in \mathcal{W}_k, u \in \mathcal{U}_l} dF(a, y, w, u) \\ &= \frac{x_{ijkl} dad y d w d u}{\text{vol}(\mathcal{A}_i) \text{vol}(\mathcal{Y}_j) \text{vol}(\mathcal{W}_k) \text{vol}(\mathcal{U}_l)}, \end{aligned}$$

$$\begin{aligned} dF(a, w, u) &\approx \frac{dad w d u}{\text{vol}(\mathcal{A}_i) \text{vol}(\mathcal{W}_k) \text{vol}(\mathcal{U}_l)} \int_{a \in \mathcal{A}_i, w \in \mathcal{W}_k, u \in \mathcal{U}_l} dF(a, w, u) \\ &= \frac{dad w d u}{\text{vol}(\mathcal{A}_i) \text{vol}(\mathcal{W}_k) \text{vol}(\mathcal{U}_l)} \int_{a \in \mathcal{A}_i, y \in \mathcal{Y}, w \in \mathcal{W}_k, u \in \mathcal{U}_l} dF(a, y, w, u) \\ &= \frac{\sum_{j'} x_{ij'kl} dad w d u}{\text{vol}(\mathcal{A}_i) \text{vol}(\mathcal{W}_k) \text{vol}(\mathcal{U}_l)}, \end{aligned}$$

$$\begin{aligned} dF(w, u) &\approx \frac{d w d u}{\text{vol}(\mathcal{W}_k) \text{vol}(\mathcal{U}_l)} \int_{w \in \mathcal{W}_k, u \in \mathcal{U}_l} dF(w, u) \\ &= \frac{d w d u}{\text{vol}(\mathcal{W}_k) \text{vol}(\mathcal{U}_l)} \int_{a \in \mathcal{A}, y \in \mathcal{Y}, w \in \mathcal{W}_k, u \in \mathcal{U}_l} dF(a, y, w, u) \\ &= \frac{\sum_{i', j'} x_{i'j'kl} d w d u}{\text{vol}(\mathcal{W}_k) \text{vol}(\mathcal{U}_l)}. \end{aligned}$$

Plugging all above equalities yields

$$\begin{aligned} &\int_{y \in \mathcal{Y}_j, w \in \mathcal{W}_k, u \in \mathcal{U}_l} y \frac{dF(a, y, w, u) dF(w, u)}{dF(a, w, u)} \\ &\approx \frac{x_{ijkl} \sum_{i', j'} x_{i'j'kl}}{\sum_{j'} x_{ij'kl}} \int_{y \in \mathcal{Y}_j, w \in \mathcal{W}_k, u \in \mathcal{U}_l} \\ &= \frac{x_{ijkl} \sum_{i', j'} x_{i'j'kl}}{\sum_{j'} x_{ij'kl}} \int_{y \in \mathcal{Y}_j, w \in \mathcal{W}_k, u \in \mathcal{U}_l} y d y d w d u / \text{vol}(\mathcal{Y}_j) \text{vol}(\mathcal{W}_k) \text{vol}(\mathcal{U}_l) \\ &\approx \frac{y_j x_{ijkl} \sum_{i', j'} x_{i'j'kl}}{\sum_{j'} x_{ij'kl}}. \end{aligned}$$

If y_j is chosen to be $\frac{\int_{y \in \mathcal{Y}_j} y d y}{\int_{y \in \mathcal{Y}_j} d y}$, then the last symbol of approximation can be replaced with the symbol of equal. If \mathcal{Y}_j is an interval, y_j can be chosen as the midpoint of \mathcal{Y}_j .

The step of approximating dF is crucial in reducing the approximation error. For absolutely continuous cumulative distribution functions, the approximation error will converge to zero as the diameter of each block approaches zero. Furthermore, if all random variables are discrete, the

approximation error can be exactly zero when using the natural discretization. In this case, the original objective can be expressed as

$$\sum_{y \in \mathcal{Y}, w \in \mathcal{W}, u \in \mathcal{U}} y \frac{\mathbb{P}(A = a, Y = y, W = w, U = u) \mathbb{P}(W = w, U = u)}{\mathbb{P}(A = a, W = w, U = u)}.$$

Our discretization method can be regarded as approximating probability mass functions.

C.3 Proof of convergence results of Algorithm 2

We first prove the following lemma to show that our sampling algorithm can cover all values in the feasible region \mathcal{D} . We denote the truncated distribution to $[l, h]$ from the user-given distribution F_s when x_i is given in sequential LPs as $F_s(x|x_i, [l, h])$.

Lemma C.1 *The Algorithm 7 induces a distribution on the given simplex \mathcal{D} .*

Proof. We need to prove the sample generated by Algorithm 7 can exactly cover the region of \mathcal{D} . On the one hand, for any output \mathbf{x} , the feasibility of each component of \mathbf{x} indicates that \mathbf{x} must lie in \mathcal{D} . On the another hand, for any $\hat{\mathbf{x}} \in \mathcal{D}$, we show that this point can be generated by solving sequential LPs. Since $\hat{\mathbf{x}} \in \mathcal{D}$, $\hat{\mathbf{x}}$ is a feasible solution to the first LP

$$\begin{aligned} & \max / \min x_1, \\ & \text{s.t. } A\mathbf{x} \leq \mathbf{b}, \mathbf{x} \geq \mathbf{0}. \end{aligned}$$

One can check the feasibility of $\hat{\mathbf{x}}$ in the following LPs

$$\begin{aligned} & \max / \min x_i, \\ & \text{s.t. } A\mathbf{x} \leq \mathbf{b}, \mathbf{x} \geq \mathbf{0}, \\ & x_1 = \hat{x}_1, \dots, x_j = \hat{x}_j, j = 1, 2, \dots, i-1, \end{aligned}$$

because $\hat{\mathbf{x}} \in \mathcal{D}$ and the previous i components are exactly equal to those of $\hat{\mathbf{x}}$.

Suppose that the number of components of $\hat{\mathbf{x}}$ is d . Then the induced distribution is

$$F(\hat{\mathbf{x}}) = F_s(x_1|[l_1, h_1]) \prod_{i=2}^d F_s(x_i|[l_i, h_i], x_j, j = 1, 2, \dots, i-1).$$

□

We now give the proof for Proposition 3.1.

Proof. The optimization problem (7) has one-to-one correspondence between \mathbf{x} and each causal model where all random variables are discrete. From Lemma C.1, we know the one-to-one correspondence between each model and \mathbf{x} . Therefore, $[l(a), h(a)]$ is the support of the induced distribution on casual bounds.

As shown in (6), the objective can be regarded as a function of \mathbf{x} . We define $\phi = \mathbb{E}_{\mathcal{M}}[Y|\text{do}(A = a)]$ which is a continuous mapping from \mathcal{D} to $[0, 1]$. The continuity of ϕ is clear for $\sum_{j'} x_{ij'kl} > 0$. When $\sum_{j'} x_{ij'kl} = 0$, the non-negativity of $x_{ij'kl}$ implies $\sum_{i', j'} x_{i'j'kl} = 0$. In this case, we can set the value of $\frac{y_j x_{ij'kl} \sum_{i', j'} x_{i'j'kl}}{\sum_{j'} x_{ij'kl}}$ to be 0 to maintain continuity.

Given that \mathcal{D} is a compact set, there exists \mathbf{x}_l such that $\phi(\mathbf{x}_l) = l(a)$. Let $b(a)$ be a sample generated by Algorithm 2. Then the continuity of ϕ indicates that $\forall \epsilon > 0$, there exists $\delta > 0$ such that $\phi(\mathbf{x}) < l(a) + \epsilon$ for all $\mathbf{x} \in \mathcal{B}(\mathbf{x}_l, \delta)$, then

$$\mathbb{P}(b(a) < l(a) + \epsilon) = \mathbb{P}_s \left(\bigcup_{b(a) < l(a) + \epsilon} \{\mathbf{x} \in \mathcal{D} | \phi(\mathbf{x}) = b(a)\} \right) \geq \mathbb{P}_s(\mathcal{B}(\mathbf{x}_l, \delta)) > 0.$$

Suppose that $b_{(1)}(a), \dots, b_{(B)}(a)$ is the ordered statistics for the output of Algorithm 2. Then we have

$$\mathbb{P}(l_B(a) < l(a) + \epsilon) = \mathbb{P}(b_{(1)}(a) < l(a) + \epsilon) = 1 - (1 - \mathbb{P}(b(a) < l(a) + \epsilon))^B \rightarrow 1$$

as $B \rightarrow \infty$. Since $l_B(a)$ is a feasible solution to the discrete optimization problem, we have

$$\mathbb{P}(l(a) \leq l_B(a) < l(a) + \epsilon) = 1 - (1 - \mathbb{P}(b(a) < l(a) + \epsilon))^B \rightarrow 1$$

which implies $l_B(a) \rightarrow l(a)$ in probability.

Similarly, we can prove that $\mathbb{P}(h_B(a) > h(a) - \epsilon) < 1$ and thus $h_B(a) \rightarrow h(a)$ in probability. \square

Proof. The one-to-one correspondence between \mathbf{x} and each causal model has been proved in Lemma C.1. Therefore, $[l(a), h(a)]$ is the support of the induced distribution on casual bounds. As shown in the proof of Proposition 3.1, the defined $\phi = \mathbb{E}_{\mathcal{M}}[Y | \text{do}(A = a)]$ is a continuous mapping from \mathcal{D} to $[0, 1]$.

Given that \mathcal{D} is a compact set, there exists \mathbf{x}_l such that $\phi(\mathbf{x}_l) = l(a)$. The property of OPT implies that there exists $\delta > 0$ such that

$$\text{OPT}(\min / \max, (6), \mathcal{D}, \mathbf{x}) = \mathbf{x}_l, \forall \mathbf{x} \in \mathcal{B}(\mathbf{x}_l, \delta) \cap \mathcal{D}.$$

Hence, we have

$$\mathbb{P}(l_B(a) = l(a)) \geq \mathbb{P}_s(\mathcal{B}(\mathbf{x}_l, \delta) \cap \mathcal{D}) > 0.$$

Due to Borel-Cantelli lemma we can prove that $l_B(a) \rightarrow l(a)$ almost surely, because each sample $b(a)$ is i.i.d. generated by Algorithm 8. Similarly, we can prove that $h_B(a) \rightarrow h(a)$ almost surely. \square

C.4 Proof of regrets in Section 3.1

We first prove Theorem 4.1.

Proof. Case 1: $h(a) < \max_{i \in \mathcal{A}} l(i)$

From the algorithmic construction, we know that such arm a is removed and thus

$$\mathbb{E}[N_a(T)] = 0.$$

Case 2: $\max_{i \in \mathcal{A}} l(i) \leq h(a) < \mu^*$.

Let $a^* = \text{argmax}_{a \in \mathcal{A}} \mathbb{E}[Y | \text{do}(A = a)]$ be the optimal action with respect to w . Define the following event

$$\mathcal{E}(t) = \left\{ \hat{\mu}_a \in \left[\mu_a - \frac{\log t}{n_a(t)}, \mu_a + \frac{\log t}{n_a(t)} \right], \forall a \in \mathcal{A} \right\}$$

Then the Chernoff's bound yields

$$\mathbb{P}(\overline{\mathcal{E}(t)}) \leq \sum_{a \in \mathcal{A}} \exp(-2n_a(t) \times \frac{\log t}{n_a(t)}) \leq \frac{|\mathcal{A}|}{t^2}$$

For any given w , the event $\{A_t = a\}$ implies $\hat{U}_a(t) > \hat{U}_{a^*}(t)$. However,

$$\mu^* > h(a) \geq \hat{U}_a(t)$$

and

$$\hat{U}_{a^*}(t) \geq \mu^*$$

if $\mathcal{E}(t)$ holds. This leads to contradiction. Therefore,

$$\begin{aligned} \mathbb{E}[N_a(T)] &= \sum_{t=1}^T \mathbb{P}(A_t = a) \\ &= \sum_{t=1}^T \mathbb{P}(A_t = a | \mathcal{E}(t)) \mathbb{P}(\mathcal{E}(t)) + \mathbb{P}(A_t = a | \overline{\mathcal{E}(t)}) \mathbb{P}(\overline{\mathcal{E}(t)}) \\ &\leq \sum_{t=1}^T \mathbb{P}(\overline{\mathcal{E}(t)}) \\ &\leq \sum_{t=1}^T \frac{|\mathcal{A}|}{t^2} \\ &\leq \frac{|\mathcal{A}| \pi^2}{6}. \end{aligned}$$

Case 3: $h(a) \geq \mu^*$

We reuse the notation $\mathcal{E}(t)$ in the case 2. Condition on the event $\bigcap_{t=1}^T \mathcal{E}(t)$, if $n_a(t) \geq \frac{8 \log T}{\Delta_a^2}$, then

$$\hat{U}_a(t) \leq U_a(t) = \mu_a + \sqrt{\frac{2 \log t}{n_a(t)}} \leq \mu_a + \frac{1}{2} \Delta_a = \mu^* \leq \hat{U}_{a^*}(t),$$

so Algorithm 5 will not choose the action a at the round t . Therefore,

$$\mathbb{E}[N_a(T)] \leq \mathbb{E} \left[N_a(T) \middle| \bigcap_{t=1}^T \mathcal{E}(t) \right] + T \mathbb{P} \left(\overline{\bigcap_{t=1}^T \mathcal{E}(t)} \right) \leq \frac{8 \log T}{\Delta_a^2} + T \mathbb{P} \left(\bigcup_{t=1}^T \overline{\mathcal{E}(t)} \right).$$

We conclude the proof by showing

$$T \mathbb{P} \left(\overline{\bigcup_{t=1}^T \mathcal{E}(t)} \right) \leq T \sum_{t=1}^T \frac{|\mathcal{A}|}{t^2} < T \times \frac{|\mathcal{A}|}{T} = |\mathcal{A}|.$$

□

Actually, the proof is just a simple modification of that in Theorem 4.2, because MAB can be regarded as a special case of contextual bandits.

Theorem C.2 Consider a MAB bandit problem with $|\mathcal{A}| < \infty$. Denote

$$\widetilde{\mathcal{A}}^* = \mathcal{A} - \{a \in \mathcal{A} | h(a) < \mu^*\}.$$

Then the regret of Algorithm 3 is upper bounded by

$$\mathbb{E}[\text{Reg}(T)] \leq \sqrt{8(|\widetilde{\mathcal{A}}^*| - 1)T \log T}.$$

Proof. Theorem 4.1 shows that

$$\begin{aligned} \mathbb{E}[\text{Reg}(T)] &= \sum_{a \in \mathcal{A}} \Delta_a \mathbb{E}[N_a(T)] \\ &\leq \sum_{a \in \widetilde{\mathcal{A}}^*} \frac{8 \log T}{\Delta_a} \mathbf{I}\{\Delta_a \geq \Delta\} + T\Delta + \mathcal{O}(|\mathcal{A}|) \\ &\leq \frac{8(|\widetilde{\mathcal{A}}^*| - 1) \log T}{\Delta} + T\Delta + \mathcal{O}(|\mathcal{A}|). \end{aligned}$$

Specifying $\Delta = \sqrt{\frac{8(|\widetilde{\mathcal{A}}^*| - 1) \log T}{T}}$ concludes the proof. \square

Denote the contextual bandit instances with prior knowledge $l(a)$ and $h(a)$ as

$$\mathfrak{M} = \{\text{MAB bandit instances with } l(a) \leq \mu_a \leq h(a), \forall a \in \mathcal{A}\}.$$

Theorem C.3 Suppose $|\mathcal{A}| < \infty$. Then for any algorithm \mathbf{A} , there exists an absolute constant $c > 0$ such that

$$\min_{\mathbf{A}} \sup_{\mathfrak{M}} \text{Reg}(T) \geq \frac{1}{27} \sqrt{(|\widetilde{\mathcal{A}}^*| - 1)T}.$$

Proof. This is a direct corollary of MAB regret lower bound, because any arm in $\widetilde{\mathcal{A}}^*$ cannot be the optimal one. \square

C.5 Proof of Proposition 2.1

Proof. From the rule of do-calculus, we have

$$\begin{aligned} \mathbb{E}[Y | \text{do}(A = a), w] &= \int_{u \in \mathcal{U}} \mathbb{E}[Y | \text{do}(A = a), w, u] dF(u) \\ &= \int_{u \in \mathcal{U}} \mathbb{E}[Y | a, w, u] dF(u). \end{aligned}$$

The last equality is due to the rule of do-calculus as W and U is sufficient to block all back-door paths from A to Y . \square

C.6 Epsilon-identification

In Section 2.2, we consider the fully identifiable case, with the objective $\mathbb{E}[Y | \text{do}(A = a), w]$. Given that the expert provides $F(a, y, w, u)$, it is possible to compute $F(y | a, w, u)$ and $F(u)$ from observation data. However, in practical scenarios, estimating $F(y | a, w, u)$ and $F(u)$ can result in

uncertainties. Recent research in causal inference, such as Li et al. (2022, 2023), has investigated the impact of estimation error from finite samples. In particular, Li et al. (2023) introduced the concept of ϵ -identification, which extends the original identification concept and accounts for the influence of estimation error from finite samples. To address this, we establish an ϵ -identification result using finite samples.

Proposition C.1 *Suppose A, Y, W , and U are all discrete random variables with bounded support. Assume that the samples are independently and identically distributed. For given a, w and each tuple (y, u) , the fraction of samples containing (y, u) is at least κ , where κ is an absolute positive constant. Then, for a sample size of $n \geq \frac{2|\mathcal{U}|^2|\mathcal{Y}|^2}{\kappa\delta^2} \ln\left(\frac{2|\mathcal{U}|\sum_{y \in \mathcal{Y}} y}{\epsilon}\right)$, one can achieve ϵ -identification for $\mathbb{E}[Y|\text{do}(A = a), w]$, meaning that $|\mathbb{E}[Y|\text{do}(A = a), w] - \hat{\mathbb{E}}[Y|\text{do}(A = a), w]| \leq \epsilon$ with probability at least $1 - \delta$. Here, $\hat{\mathbb{E}}[Y|\text{do}(A = a), w]$ is the sample estimate of the causal effect.*

Proof. In the discrete setting, the causal effect can be written as

$$\mathbb{E}[Y|\text{do}(A = a), w] = \sum_{u \in \mathcal{U}, y \in \mathcal{Y}} y \mathbb{P}(y|a, w, u) \mathbb{P}(u).$$

The sample size of $\hat{\mathbb{P}}(u)$ and $\hat{\mathbb{P}}(y|a, w, u)$ is at least κn . Due to i.d.d. assumption of each tuple (y, u) and Hoeffding's inequality, then with probability at least $1 - \delta/(2|\mathcal{U}||\mathcal{Y}|)$, we have

$$|\hat{\mathbb{P}}(u) - \mathbb{P}(u)| \leq \exp(-\kappa n \delta^2 / (2|\mathcal{U}|^2|\mathcal{Y}|^2)), |\hat{\mathbb{P}}(y|a, w, u) - \mathbb{P}(y|a, w, u)| \leq \exp(-\kappa n \delta^2 / (2|\mathcal{U}|^2|\mathcal{Y}|^2)).$$

Therefore, since

$$\hat{\mathbb{E}}[Y|\text{do}(A = a), w] = \sum_{u \in \mathcal{U}, y \in \mathcal{Y}} y \hat{\mathbb{P}}(y|a, w, u) \hat{\mathbb{P}}(u),$$

with probability at least $1 - \delta$, we have

$$\begin{aligned} & |\hat{\mathbb{E}}[Y|\text{do}(A = a), w] - \mathbb{E}[Y|\text{do}(A = a), w]| \\ &= \left| \sum_{u \in \mathcal{U}, y \in \mathcal{Y}} y (\hat{\mathbb{P}}(y|a, w, u) \hat{\mathbb{P}}(u) - \mathbb{P}(y|a, w, u) \mathbb{P}(u)) \right| \\ &\leq \sum_{u \in \mathcal{U}, y \in \mathcal{Y}} y |\hat{\mathbb{P}}(y|a, w, u) \hat{\mathbb{P}}(u) - \mathbb{P}(y|a, w, u) \mathbb{P}(u)| \\ &\leq \sum_{u \in \mathcal{U}, y \in \mathcal{Y}} y (|\hat{\mathbb{P}}(y|a, w, u) - \mathbb{P}(y|a, w, u)| \mathbb{P}(u) + \hat{\mathbb{P}}(y|a, w, u) |\hat{\mathbb{P}}(u) - \mathbb{P}(u)|) \\ &\leq 2|\mathcal{U}| \left(\sum_{y \in \mathcal{Y}} y \right) \exp(-\kappa n \delta^2 / (2|\mathcal{U}|^2|\mathcal{Y}|^2)). \end{aligned}$$

Let the RHS be equal to ϵ . Then we have

$$n \geq \frac{2|\mathcal{U}|^2|\mathcal{Y}|^2}{\kappa\delta^2} \ln\left(\frac{2|\mathcal{U}|\sum_{y \in \mathcal{Y}} y}{\epsilon}\right).$$

□

C.7 Theorems in Task 2

Theorem C.4 *Given a causal diagram \mathcal{G} and a distribution compatible with \mathcal{G} , let (W, U) be a set of variables satisfying the back-door criterion in \mathcal{G} relative to an ordered pair (A, Y) , where (W, U) is partially observable, i.e., only probabilities $\hat{F}(a, y, w)$ and $\hat{F}(u)$ with the maximum estimation error ϵ , the causal effects of $A = a_0$ on Y when $W = w_0$ occurs are then bounded as follows:*

$$l(a_0, w_0) \leq \mathbb{E}[Y | \text{do}(A = a_0), w_0] \leq h(a_0, w_0),$$

where $l(w_0, a_0)$ and $h(w_0, a_0)$ are solutions to the following functional optimization problem for any given a_0 and w_0

$$\begin{aligned} l(a_0, w_0) &= \inf \int_{w \in \mathcal{W}, u \in \mathcal{U}} \int_{y \in \mathcal{Y}} y dF(y | a_0, w_0, u) dF(u) \\ h(a_0, w_0) &= \sup \int_{w \in \mathcal{W}, u \in \mathcal{U}} \int_{y \in \mathcal{Y}} y dF(y | a_0, w_0, u) dF(u) \\ \text{s.t. } &F(y | a, w, u) F(a, w, u) = F(a, y, w, u), \forall (a, y, w, u) \in \mathcal{A} \times \mathcal{Y} \times \mathcal{W} \times \mathcal{U} \\ &\int_{y \in \mathcal{Y}} dF(a, y, w, u) = F(a, w, u), \forall (a, w, u) \in \mathcal{A} \times \mathcal{W} \times \mathcal{U} \\ &\int_{a \in \mathcal{A}, y \in \mathcal{Y}, w \in \mathcal{W}} dF(a, y, w, u) = F(u), \forall u \in \mathcal{U} \\ &\int_{u \in \mathcal{U}} dF(a, y, w, u) = F(a, y, w), \forall (a, y, w) \in \mathcal{A} \times \mathcal{Y} \times \mathcal{W} \\ &|F(a, y, w) - \hat{F}(a, y, w)| \leq \epsilon, \forall (a, y, w) \in \mathcal{A} \times \mathcal{Y} \times \mathcal{W} \\ &|F(u) - \hat{F}(u)| \leq \epsilon, \forall u \in \mathcal{U}. \end{aligned}$$

Here the inf/sup is taken with respect to all unknown cumulative distribution functions $F(a, y, w, u)$, $F(a, y, w)$, $F(a, w, u)$, $F(u)$.

Proof. The object is shown in the proof of Proposition 2.1. The equalities come from the normalization properties, and inequalities follow from estimation error. \square

Denote the following optimization problem

$$\begin{aligned} &\max / \min \hat{\mathbb{E}}_{\mathcal{M}}[Y | \text{do}(A = a), w] \\ \text{s.t. } &\sum_l x_{ijkl} = \theta_{ijk}, \forall i \in [n_{\mathcal{A}}], j \in [n_{\mathcal{Y}}], k \in [n_{\mathcal{W}}] \\ &\sum_{ijk} x_{ijkl} = \theta_l, \forall l \in [n_{\mathcal{U}}]. \end{aligned} \tag{20}$$

where the objective $\hat{\mathbb{E}}_{\mathcal{M}}[Y | \text{do}(A = a), w]$ after discretization is defined as

$$\hat{\mathbb{E}}_{\mathcal{M}}[Y | \text{do}(A = a), w] = \sum_{jkl} \frac{y_j \theta_l x_{ijkl}}{\sum_{j'} x_{ij'kl}}. \tag{21}$$

Denote the solutions to (20) as $l(a, w)$ and $h(a, w)$. Note that the optimization problem (13) shares the same feasible region with that of (4).

Proposition C.2 Assume that the sampling measure \mathbb{P}_s satisfies $\forall \mathbf{x} \in \mathcal{D}$, and $\forall \delta > 0$,

$$\mathbb{P}_s(\mathcal{B}(\mathbf{x}, \delta) \cap \mathcal{D}) > 0,$$

where $\mathcal{B}(\mathbf{x}, \delta)$ is a ball centered at \mathbf{x} with radius δ . Then $l_B(a, w)$ and $h_B(a, w)$ converge in probability to $l(a, w)$ and $h(a, w)$ for $B \rightarrow \infty$, respectively.

Proof. As shown in (14), the object can also be regarded as a function of \mathbf{x} . We define $\phi = \hat{\mathbb{E}}_{\mathcal{M}}[Y | \text{do}(A = a), w]$ which is a continuous mapping from \mathcal{D} to $[0, 1]$. The continuity of ϕ holds similarly.

Given that \mathcal{D} is a compact set, there exists \mathbf{x}_l such that $\phi(\mathbf{x}_l) = l(a, w)$. Suppose that $b(a, w)$ is a sample generated by Algorithm 4. The continuity of ϕ indicates that $\forall \epsilon > 0$, there exists $\delta > 0$ such that $\phi(\mathbf{x}) < l(a, w) + \epsilon$ for all $\mathbf{x} \in \mathcal{B}(\mathbf{x}_l, \delta)$, then

$$\mathbb{P}(b(a, w) < l(a, w) + \epsilon) = \mathbb{P}_s \left(\bigcup_{b < l(a, w) + \epsilon} \{\mathbf{x} \in \mathcal{D} | \phi(\mathbf{x}) = b\} \right) \geq \mathbb{P}_s(\mathcal{B}(\mathbf{x}_l, \delta)) > 0.$$

This implies that

$$\mathbb{P}(b_{(1)}(a, w) < l(a, w) + \epsilon) = 1 - (1 - \mathbb{P}(b(a, w) < l(a, w) + \epsilon))^B \rightarrow 1$$

as $B \rightarrow \infty$. Since $b_{(1)}(a, w)$ is a feasible solution to the discrete optimization problem, we have

$$\mathbb{P}(l(a, w) \leq b_{(1)}(a, w) < l(a, w) + \epsilon) = 1 - (1 - \mathbb{P}(b(a, w) < l(a, w) + \epsilon))^B \rightarrow 1$$

which implies $l_B(a, w) \rightarrow l(a, w)$ in probability.

Similarly, we can prove that $\mathbb{P}(b_{(B)}(a, w) > h(a, w) - \epsilon) < 1$ and thus $h_B(a, w) \rightarrow h(a, w)$ in probability. □

We can also incorporate the optimization procedure `OPT`. Let the objective in Algorithm 8 be (14). We can also prove the similar almost surely convergence result.

Proposition C.3 Assume that the sampling measure \mathbb{P}_s satisfies $\forall \mathbf{x} \in \mathcal{D}$, and $\forall \delta > 0$,

$$\mathbb{P}_s(\mathcal{B}(\mathbf{x}, \delta) \cap \mathcal{D}) > 0,$$

where $\mathcal{B}(\mathbf{x}, \delta)$ is a ball centered at \mathbf{x} with radius δ . Given a deterministic procedure `OPT` which satisfies for any local optima \mathbf{x}_{loc} , there exists $\delta > 0$ such that for any initial guess $\mathbf{x}_0 \in \mathcal{B}(\mathbf{x}_{loc}, \delta) \cap \mathcal{D}$, `OPT` can output \mathbf{x}_{loc} as a result. Suppose that $l_B(a, w)$ and $h_B(a, w)$ are the outputs of Algorithm 8 with the target (14). Then $l_B(a, w)$ and $h_B(a, w)$ converge almost surely to $l(a, w)$ and $h(a, w)$ for $B \rightarrow \infty$, respectively.

Proof. The one-to-one correspondence between \mathbf{x} and each causal model has been proved in Lemma C.1. Therefore, $[l(a, w), h(a, w)]$ is the support of the induced distribution on causal bounds. As shown in the proof of Proposition 3.1, the defined $\phi = \mathbb{E}_{\mathcal{M}}[Y | \text{do}(A = a), w]$ is a continuous mapping from \mathcal{D} to $[0, 1]$.

Given that \mathcal{D} is a compact set, there exists \mathbf{x}_l such that $\phi(\mathbf{x}_l) = l(a, w)$. The property of OPT implies that there exists $\delta > 0$ such that

$$\text{OPT}(\min / \max, (6), \mathcal{D}, \mathbf{x}) = \mathbf{x}_l, \forall \mathbf{x} \in \mathcal{B}(\mathbf{x}_l, \delta) \cap \mathcal{D}.$$

Hence, we have

$$\mathbb{P}(b(a, w) = l(a, w)) \geq \mathbb{P}_s(\mathcal{B}(\mathbf{x}_l, \delta) \cap \mathcal{D}) > 0.$$

Due to Borel-Cantelli lemma we can prove that $l_B(a, w) \rightarrow l(a, w)$ almost surely, because each $b_i(a, w)$ is independently sampled by Algorithm 8. Similarly, we can prove that $h_B(a, w) \rightarrow h(a, w)$ almost surely. □

C.8 Proof of Theorem 4.2

Proof. We consider any given w in the following proof.

Case 1: $h(a, w) < \max_{i \in \mathcal{A}} l(i, w)$

From the algorithmic construction, we know that such arm a is removed and thus

$$\mathbb{E}[N_a(T_w)] = 0.$$

Case 2: $\max_{i \in \mathcal{A}} l(i, w) \leq h(a, w) < \mu_w^*$.

Let $a_w^* = \text{argmax}_{a \in \mathcal{A}} \mathbb{E}[Y | \text{do}(A = a), w]$ be the optimal action with respect to w . Define the following event

$$\mathcal{E}_w(t) = \left\{ \hat{\mu}_{a,w} \in \left[\mu_{a,w} - \frac{\log t}{n_{a,w}(t)}, \mu_{a,w} + \frac{\log t}{n_{a,w}(t)} \right], \forall a \in \mathcal{A} \right\}$$

Then the Chernoff's bound yields

$$\mathbb{P}(\overline{\mathcal{E}_w(t)}) \leq \sum_{a \in \mathcal{A}} \exp\left(-2n_{a,w}(t) \times \frac{\log t}{n_{a,w}(t)}\right) \leq \frac{|\mathcal{A}|}{t^2}$$

For any given w , the event $\{A_t = a\}$ implies $\hat{U}_{a,w}(t) > \hat{U}_{a,w^*}(t)$. However,

$$\mu_w^* > h(a, w) \geq \hat{U}_{a,w}(t)$$

and

$$\hat{U}_{a,w^*}(t) \geq \mu_w^*$$

if $\mathcal{E}_w(t)$ holds. This leads to contradiction. Therefore,

$$\begin{aligned}
\mathbb{E}[N_a(T_w)] &= \sum_{t=1}^{T_w} \mathbb{P}(A_t = a | w_t = w) \\
&= \sum_{t=1}^{T_w} \mathbb{P}(A_t = a | w_t = w, \mathcal{E}_w(t)) \mathbb{P}(\mathcal{E}_w(t)) + \mathbb{P}(A_t = a | w_t = w, \overline{\mathcal{E}_w(t)}) \mathbb{P}(\overline{\mathcal{E}_w(t)}) \\
&\leq \sum_{t=1}^{T_w} \mathbb{P}(\overline{\mathcal{E}_w(t)}) \\
&\leq \sum_{t=1}^{T_w} \frac{|\mathcal{A}|}{t^2} \\
&\leq \frac{|\mathcal{A}|\pi^2}{6}.
\end{aligned}$$

Case 3: $h(a, w) \geq \mu_w^*$

We reuse the notation $\mathcal{E}_w(t)$ in the case 2. Condition on the event $\bigcap_{t=1}^{T_w} \mathcal{E}_w(t)$, if $n_{a,w}(t) \geq \frac{8 \log T_w}{\Delta_{a,w}^2}$, then

$$\hat{U}_{a,w}(t) \leq U_{a,w}(t) = \mu_{a,w} + \sqrt{\frac{2 \log t}{n_{a,w}(t)}} \leq \mu_{a,w} + \frac{1}{2} \Delta_{a,w} = \mu_w^* \leq \hat{U}_{a,w^*}(t),$$

so Algorithm 5 will not choose the action a at the round t . Therefore,

$$\mathbb{E}[N_a(T_w)] \leq \mathbb{E} \left[N_a(T_w), \bigcap_{t=1}^{T_w} \mathcal{E}_w(t) \right] + T_w \mathbb{P} \left(\bigcap_{t=1}^{T_w} \overline{\mathcal{E}_w(t)} \right) \leq \frac{8 \log T_w}{\Delta_{a,w}^2} + T_w \mathbb{P} \left(\bigcup_{t=1}^{T_w} \overline{\mathcal{E}_w(t)} \right).$$

We conclude the proof by showing

$$T_w \mathbb{P} \left(\bigcup_{t=1}^{T_w} \overline{\mathcal{E}_w(t)} \right) \leq T_w \sum_{t=1}^{T_w} \frac{|\mathcal{A}|}{t^2} < T_w \times \frac{|\mathcal{A}|}{T_w} = |\mathcal{A}|.$$

□

C.9 Proof of Theorem 4.3

Proof. Let Δ_w be the constant with respect to w that we will specify later. From the proof of Theorem 4.2, we know that the expected regret can be upper bounded as

$$\begin{aligned}
\mathbb{E}[\text{Reg}(T)] &= \sum_{w \in \mathcal{W}} \sum_{a \in \mathcal{A}} \Delta_{a,w} \mathbb{E}[N_a(T_w)] \\
&\leq \sum_{w \in \mathcal{W}} \left(\sum_{a \in \tilde{\mathcal{A}}^*(w)} \frac{8 \log T_w}{\Delta_{a,w}} \mathbf{I} \{ \Delta_{a,w} \geq \Delta_w \} + T \Delta_w \right) + \mathcal{O}(|\mathcal{A}|) \\
&\leq \sum_{w \in \mathcal{W}} \left(\frac{8(|\tilde{\mathcal{A}}^*(w)| - 1) \log T}{\Delta_w} + T \Delta_w \right) + \mathcal{O}(|\mathcal{A}|).
\end{aligned}$$

We select $\Delta_w = \sqrt{\frac{8|\widetilde{\mathcal{A}}^*(w)| \log T}{T_w}}$ so

$$\mathbb{E}[\text{Reg}(T)] \leq \sum_{w \in \mathcal{W}} \sqrt{8(|\widetilde{\mathcal{A}}^*(w)| - 1)T_w \log T}.$$

By strong law of large numbers, we have

$$\begin{aligned} \limsup_{T \rightarrow \infty} \frac{\mathbb{E}[\text{Reg}(T)]}{\sqrt{T \log T}} &\leq \sum_{w \in \mathcal{W}} \sqrt{8(|\widetilde{\mathcal{A}}^*(w)| - 1) \limsup_{T \rightarrow \infty} \frac{T_w}{T}} \\ &= \sum_{w \in \mathcal{W}} \sqrt{8(|\widetilde{\mathcal{A}}^*(w)| - 1) \mathbb{P}(W = w)}. \end{aligned}$$

□

Proof. Consider $|\mathcal{W}|$ MAB instances. For any given context w , the set that the optimal arm will be in is $\mathcal{A}^*(w)$. For any algorithm \mathbf{A} , let \mathbf{A}_w be the induced algorithm of \mathbf{A} when w occurs. From the minimax theorem for MAB instances Lattimore and Szepesvári (2020), we know that there exists a MAB instance for each w such that the regret of \mathbf{A}_w is at least $\frac{1}{27} \sqrt{(|\widetilde{\mathcal{A}}^*(w)| - 1)T_w}$, where T_w is the number of occurrence of w . Hence,

$$\text{Reg}(T) \geq \sum_{w \in \mathcal{W}} \frac{1}{27} \sqrt{(|\widetilde{\mathcal{A}}^*(w)| - 1)T_w}.$$

and thus

$$\begin{aligned} \limsup_{T \rightarrow \infty} \frac{\text{Reg}(T)}{\sqrt{T}} &\geq \frac{1}{27} \sum_{w \in \mathcal{W}} \sqrt{(|\widetilde{\mathcal{A}}^*(w)| - 1) \cdot \limsup_{T \rightarrow \infty} \frac{T_w}{T}} \\ &= \frac{1}{27} \sum_{w \in \mathcal{W}} \sqrt{(|\widetilde{\mathcal{A}}^*(w)| - 1) \mathbb{P}(W = w)}. \end{aligned}$$

□

C.10 Proof of Theorem 4.5

The framework presented in Foster et al. (2020), Simchi-Levi and Xu (2022) provides a method to analyze contextual bandit algorithms in the universal policy space Ψ . In this paper, we mainly focus on a subspace of Ψ shaped by causal bounds. We demonstrate that the action distribution p_m selected in Algorithm 6 possesses desirable properties that contribute to achieving low regrets.

For each epoch m and any round t in epoch m , for any possible realization of γ_t, \hat{f}_m , we define the universal policy space of Ψ :

$$\Psi = \prod_{w \in \mathcal{W}} \mathcal{A}^*(w).$$

With abuse of notations, we define

$$\mathcal{R}(\pi) = \mathbb{E}_W[f^*(\pi(W), W)] \text{ and } \text{Reg}(\pi) = \mathcal{R}(\pi_{f^*}) - \mathcal{R}(\pi).$$

The above quantities do not depend on specific values of W . The following empirical version of above quantities are defined as

$$\widehat{\mathcal{R}}_t(\pi) = \hat{f}_{m(t)}(\pi(w), w) \text{ and } \widehat{\text{Reg}}_t(\pi) = \mathbb{E}_W \left[\widehat{\mathcal{R}}_t(\pi_{\hat{f}_{m(t)}}) - \widehat{\mathcal{R}}_t(\pi) \right],$$

where $m(t)$ is the epoch of the round t .

Let $Q_m(\cdot)$ be the equivalent policy distribution for $p_m(\cdot|w)$, i.e.,

$$Q_m(\pi) = \prod_{w \in \mathcal{W}} p_m(\pi(w)|w), \forall \pi \in \Psi.$$

The existence and uniqueness of such measure $Q_m(\cdot)$ is a corollary of Kolmogorov's extension theorem. Note that both Ψ and $Q_m(\cdot)$ are $\mathcal{H}_{\tau_{m-1}}$ -measurable, where \mathcal{H}_t is the filtration up to the time t . We refer to Section 3.2 of Simchi-Levi and Xu (2022) for more detailed intuition for $Q_m(\cdot)$ and proof of existence. By Lemma 4 of Simchi-Levi and Xu (2022), we know that for all epoch m and all rounds t in epoch m , we can rewrite the expected regret in terms of our notations as

$$\mathbb{E}[\text{Reg}(T)] = \sum_{\pi \in \Psi} Q_m(\pi) \text{Reg}(\pi).$$

For simplicity, we define an epoch-dependent quantities

$$\rho_1 = 1, \rho_m = \sqrt{\frac{\eta \tau_{m-1}}{\log(2\delta^{-1}|\mathcal{F}^*| \log T)}}, m \geq 2,$$

so $\gamma_t = \sqrt{|\mathcal{A}^*(w_t)|} \rho_{m(t)}$ for $m(t) \geq 2$.

Lemma C.2 (*Implicit Optimization Problem*). *For all epoch m and all rounds t in epoch m , Q_m is a feasible solution to the following implicit optimization problem:*

$$\sum_{\pi \in \Psi} Q_m(\pi) \widehat{\text{Reg}}_t(\pi) \leq \mathbb{E}_W[\sqrt{|\mathcal{A}^*(W)|}] / \rho_m \quad (22)$$

$$\mathbb{E}_W \left[\frac{1}{p_m(\pi(W)|W)} \right] \leq \mathbb{E}_W[\mathcal{A}^*(W)] + \mathbb{E}_W[\sqrt{|\mathcal{A}^*(W)|}] \rho_m \widehat{\text{Reg}}_t(\pi), \forall \pi \in \Psi. \quad (23)$$

Proof. Let m and t in epoch m be fixed. Denote $\mathcal{P}(W)$ as the context distribution. We have

$$\begin{aligned} & \sum_{\pi \in \Psi} Q_m(\pi) \widehat{\text{Reg}}_t(\pi) \\ &= \sum_{\pi \in \Psi} Q_m(\pi) \mathbb{E}_{w_t} \left[(\hat{f}_m(\pi_{\hat{f}_m}(w_t), w_t) - \hat{f}_m(\pi(w_t), w_t)) \right] \\ &= \mathbb{E}_{w_t \sim \mathcal{P}(W)} \left[\sum_{a \in \mathcal{A}^*(w_t)} \sum_{\pi \in \Psi} \mathbf{I}\{\pi(w_t) = a\} Q_m(\pi) (\hat{f}_m(\pi_{\hat{f}_m}(w_t), w_t) - \hat{f}_m(a, w_t)) \right] \\ &= \mathbb{E}_{w_t \sim \mathcal{P}(W)} \left[\sum_{a \in \mathcal{A}^*(w_t)} p_m(a|w_t) (\hat{f}_m(\pi_{\hat{f}_m}(w_t), w_t) - \hat{f}_m(a, w_t)) \right]. \end{aligned}$$

The first and second equalities are the definitions of $\widehat{\text{Reg}}_t(\pi)$ and $Q_m(\pi)$, respectively.

Now for the context w_t , we have

$$\begin{aligned}
& \sum_{a \in \mathcal{A}^*(w_t)} p_m(a|w) (\hat{f}_m(\pi_{\hat{f}_m}(w_t), w_t) - \hat{f}_m(a, w_t)) \\
&= \sum_{a \in \mathcal{A}^*(w_t) - \{\pi_{\hat{f}_m}(w_t)\}} \frac{\hat{f}_m(\pi_{\hat{f}_m}(w_t), w_t) - \hat{f}_m(a, w_t)}{|\mathcal{A}^*(w_t)| + \gamma_t (\hat{f}_m(\pi_{\hat{f}_m}(w_t), w_t) - \hat{f}_m(a, w_t))} \\
&\leq [|\mathcal{A}^*(w_t)| - 1] / \gamma_t \\
&\leq \sqrt{|\mathcal{A}^*(w_t)|} / \rho_m.
\end{aligned}$$

We plug in the above term and apply the i.d.d. assumption on w_t to conclude the proof of the first inequality.

For the second inequality, we first observe that for any policy $\pi \in \Psi$, given any context $w \in \mathcal{W}$,

$$\frac{1}{p_m(\pi(w)|w)} = |\mathcal{A}^*(w)| + \gamma_t (\hat{f}_m(\pi_{\hat{f}_m}(w), w) - \hat{f}_m(a, w)),$$

if $a \neq \pi_{\hat{f}_m}(w)$, and

$$\frac{1}{p_m(\pi(w)|w)} \leq \frac{1}{1/|\mathcal{A}^*(w)|} = |\mathcal{A}^*(w)| + \gamma_t (\hat{f}_m(\pi_{\hat{f}_m}(w), w) - \hat{f}_m(a, w)),$$

if $a = \pi_{\hat{f}_m}(w)$. The result follows immediately by taking expectation over w . \square

Compared with IOP in Simchi-Levi and Xu (2022), the key different part is that $\mathbb{E}_W[|\mathcal{A}^*(W)|]$ is replaced by the cardinality $|\mathcal{A}|$ of the whole action set. Another different part is the universal policy space Ψ . We define Ψ as $\prod_{w \in \mathcal{W}} \mathcal{A}^*(w)$ rather than $\prod_{w \in \mathcal{W}} \mathcal{A}$. These two points highlight the adaptivity to contexts and show how causal bound affects the action selection.

Define the following high-probability event

$$\Gamma = \left\{ \forall m \geq 2, \frac{1}{\tau_{m-1}} \sum_{t=1}^{\tau_{m-1}} \mathbb{E}_{a_t, w_t} [(\hat{f}_{m(t)}(a_t, w_t) - f^*(a_t, w_t))^2 | \mathcal{H}_{t-1}] \leq \frac{1}{\rho_m^2} \right\}.$$

The high-probability event and its variants have been proved in literatures Foster et al. (2018, 2020), Simchi-Levi and Xu (2022). Our result is slightly different from them as the whole function space is eliminated to \mathcal{F}^* . Since these results share the same form, it is straightforward to show Γ holds with probability at least $1 - \delta/2$. This is the result of the union bound and the property of the **Least Square Oracle** that is independent of algorithm design.

Our setting do not change the proof procedure of the following lemma Simchi-Levi and Xu (2022), because this lemma does not explicitly involve the number of action set. This lemma bounds the prediction error between the true reward and the estimated reward.

Lemma C.3 *Assume Γ holds. For all epochs $m > 1$, all rounds t in epoch m , and all policies $\pi \in \Psi$, then*

$$\left| \widehat{\mathcal{R}}_t(\pi) - \mathcal{R}_t(\pi) \right| \leq \frac{1}{2\rho_m} \sqrt{\max_{1 \leq m' \leq m-1} \mathbb{E}_W \left[\frac{1}{p_{m'}(\pi(W)|W)} \right]}.$$

The third step is to show that the one-step regret $Reg_t(\pi)$ is close to the one-step estimated regret $\widehat{Reg}_t(\pi)$. The following lemma states the result.

Lemma C.4 *Assume Γ holds. Let $c_0 = 5.15$. For all epochs m and all rounds t in epoch m , and all policies $\pi \in \Psi$,*

$$Reg(\pi) \leq 2\widehat{Reg}_t(\pi) + c_0\sqrt{\mathbb{E}_W[\mathcal{A}^*(W)]}/\rho_m, \quad (24)$$

$$\widehat{Reg}_t(\pi) \leq 2Reg(\pi) + c_0\sqrt{\mathbb{E}_W[\mathcal{A}^*(W)]}/\rho_m. \quad (25)$$

Proof. We prove this lemma via induction on m . It is easy to check

$$Reg(\pi) \leq 1, \widehat{Reg}_t(\pi) \leq 1,$$

as $\gamma_1 = 1$ and $c_0\mathbb{E}_W[\mathcal{A}^*(W)] \geq 1$. Hence, the base case holds.

For the inductive step, fix some epoch $m > 1$ and assume that for all epochs $m' < m$, all rounds t' in epoch m' , and all $\pi \in \Psi$, the inequalities (24) and (25) hold. We first show that for all rounds t in epoch m and all $\pi \in \Psi$,

$$Reg(\pi) \leq 2\widehat{Reg}_t(\pi) + c_0\sqrt{\mathbb{E}_W[\mathcal{A}^*(W)]}/\rho_m.$$

We have

$$\begin{aligned} & Reg(\pi) - \widehat{Reg}_t(\pi) \\ &= [\mathcal{R}(\pi_{f^*}) - \mathcal{R}(\pi)] - [\widehat{\mathcal{R}}_t(\pi_{\hat{f}_m}) - \widehat{\mathcal{R}}_t(\pi)] \\ &\leq [\mathcal{R}(\pi_{f^*}) - \mathcal{R}(\pi)] - [\widehat{\mathcal{R}}_t(\pi_{f^*}) - \widehat{\mathcal{R}}_t(\pi)] \\ &\leq |\mathcal{R}(\pi_{f^*}) - \widehat{\mathcal{R}}_t(\pi_{f^*})| + |\mathcal{R}(\pi) - \widehat{\mathcal{R}}_t(\pi)| \\ &\leq \frac{1}{\rho_m} \sqrt{\max_{1 \leq m' \leq m-1} \mathbb{E}_W \left[\frac{1}{p_{m'}(\pi_{f^*}(W)|W)} \right]} + \frac{1}{\rho_m} \sqrt{\max_{1 \leq m' \leq m-1} \mathbb{E}_W \left[\frac{1}{p_{m'}(\pi(W)|W)} \right]} \\ &\leq \frac{\max_{1 \leq m' \leq m-1} \mathbb{E}_W \left[\frac{1}{p_{m'}(\pi_{f^*}(W)|W)} \right]}{5\rho_m \sqrt{\mathbb{E}_W[\mathcal{A}^*(W)]}} + \frac{\max_{1 \leq m' \leq m-1} \mathbb{E}_W \left[\frac{1}{p_{m'}(\pi(W)|W)} \right]}{5\rho_m \sqrt{\mathbb{E}_W[\mathcal{A}^*(W)]}} + \frac{5\sqrt{\mathbb{E}_W[\mathcal{A}^*(W)]}}{8\rho_m}. \end{aligned}$$

The last inequality is by the AM-GM inequality. There exists an epoch i such that

$$\max_{1 \leq m' \leq m-1} \mathbb{E}_W \left[\frac{1}{p_{m'}(\pi(W)|W)} \right] = \mathbb{E}_W \left[\frac{1}{p_i(\pi(W)|W)} \right].$$

From Lemma C.2 we know that

$$\mathbb{E}_W \left[\frac{1}{p_i(\pi(W)|W)} \right] \leq \mathbb{E}_W[\mathcal{A}^*(W)] + \mathbb{E}_W[\sqrt{|\mathcal{A}^*(W)|}] \rho_i \widehat{Reg}_t(\pi),$$

holds for all $\pi \in \Psi$, for all epoch $1 \leq i \leq m-1$ and for all rounds t in corresponding epochs.

Hence, for epoch i and all rounds t in this epoch, we have

$$\begin{aligned}
& \frac{\max_{1 \leq m' \leq m-1} \mathbb{E}_W \left[\frac{1}{p_{m'}(\pi(W)|W)} \right]}{5\rho_m \sqrt{\mathbb{E}_W[\mathcal{A}^*(W)]}} \\
&= \frac{\mathbb{E}_W \left[\frac{1}{p_i(\pi_{f^*}(W)|W)} \right]}{5\rho_m \sqrt{\mathbb{E}_W[\mathcal{A}^*(W)]}}, \text{ (Lemma C.2:(25))} \\
&\leq \frac{\mathbb{E}_W[\mathcal{A}^*(W)] + \mathbb{E}_W[\sqrt{|\mathcal{A}^*(W)|}] \rho_i \widehat{\text{Reg}}_t(\pi)}{5\sqrt{\mathbb{E}_W[\mathcal{A}^*(W)]} \rho_m}, \text{ (inductive assumption)} \\
&\leq \frac{\mathbb{E}_W[\mathcal{A}^*(W)] + \mathbb{E}_W[\sqrt{|\mathcal{A}^*(W)|}] \rho_i [2\text{Reg}(\pi) + c_0 \sqrt{\mathbb{E}_W[\mathcal{A}^*(W)]} / \rho_i]}{5\sqrt{\mathbb{E}_W[\mathcal{A}^*(W)]} \rho_m}, \text{ (Jensen's inequality)} \\
&\leq \frac{\mathbb{E}_W[\mathcal{A}^*(W)] + \sqrt{\mathbb{E}_W[|\mathcal{A}^*(W)|]} \rho_i [2\text{Reg}(\pi) + c_0 \sqrt{\mathbb{E}_W[\mathcal{A}^*(W)]} / \rho_i]}{5\sqrt{\mathbb{E}_W[\mathcal{A}^*(W)]} \rho_m}, \text{ } (\rho_i \leq \rho_m \text{ for } i \leq m) \\
&\leq \frac{2}{5} \text{Reg}(\pi) + \frac{1+c_0}{5\rho_m} \sqrt{\mathbb{E}_W[|\mathcal{A}^*(W)|]}.
\end{aligned}$$

We can bound $\frac{\max_{1 \leq m' \leq m-1} \mathbb{E}_W \left[\frac{1}{p_{m'}(\pi(W)|W)} \right]}{5\rho_m \sqrt{\mathbb{E}_W[\mathcal{A}^*(W)]}}$ in the same way.

Combing all above inequalities yields

$$\begin{aligned}
\text{Reg}(\pi) - \widehat{\text{Reg}}_t(\pi) &\leq \frac{2(1+c_0)\sqrt{\mathbb{E}_W[\mathcal{A}^*(W)]}}{5\rho_m} + \frac{4}{5} \widehat{\text{Reg}}_t(\pi) + \frac{5\sqrt{\mathbb{E}_W[\mathcal{A}^*(W)]}}{8\rho_m} \\
&\leq \widehat{\text{Reg}}_t(\pi) + \left(\frac{2(1+c_0)}{5} + \frac{5}{8} \right) \frac{\sqrt{\mathbb{E}_W[\mathcal{A}^*(W)]}}{\rho_m} \\
&\leq \widehat{\text{Reg}}_t(\pi) + c_0 \frac{\sqrt{\mathbb{E}_W[\mathcal{A}^*(W)]}}{\rho_m}.
\end{aligned}$$

Similarly, we have

$$\begin{aligned}
& \widehat{\text{Reg}}_t(\pi) - \text{Reg}(\pi) \\
&= [\widehat{\mathcal{R}}_t(\pi_{\hat{f}_m}) - \widehat{\mathcal{R}}_t(\pi)] - [\mathcal{R}(\pi_{f^*}) - \mathcal{R}(\pi)] \\
&\leq [\widehat{\mathcal{R}}_t(\pi_{\hat{f}_m}) - \widehat{\mathcal{R}}_t(\pi)] - [\mathcal{R}(\pi_{\hat{f}_m}) - \mathcal{R}(\pi)] \\
&\leq |\mathcal{R}(\pi_{\hat{f}_m}) - \widehat{\mathcal{R}}_t(\pi_{\hat{f}_m})| + |\mathcal{R}(\pi) - \widehat{\mathcal{R}}_t(\pi)|.
\end{aligned}$$

We can bound the above terms in the same steps. □

Proof. Our regret analysis builds on the framework in Simchi-Levi and Xu (2022).

Step 1: proving an implicit optimization problem for Q_m in Lemma C.2.

Step 2: bounding the prediction error between $\widehat{\mathcal{R}}_t(\pi)$ and $\mathcal{R}_t(\pi)$ in Lemma C.3. Then we can show that the one-step regrets $\widehat{\text{Reg}}_t(\pi)$ and $\text{Reg}(\pi)$ are close to each other.

Step 3: bounding the cumulative regret $\text{Reg}(T)$.

By Lemma 4 of Simchi-Levi and Xu (2022),

$$\mathbb{E}[\text{Reg}(T)] = \sum_{t=1}^T \sum_{\pi \in \Psi} Q_{m(t)}(\pi) \text{Reg}(\pi).$$

From Lemma C.4, we know

$$\text{Reg}(\pi) \leq 2\widehat{\text{Reg}}_t(\pi) + c_0 \sqrt{\mathbb{E}_W[\mathcal{A}^*(W)]} / \rho_m$$

so

$$\begin{aligned} \mathbb{E}[\text{Reg}(T)] &= \sum_{t=1}^T \sum_{\pi \in \Psi} Q_{m(t)}(\pi) \text{Reg}(\pi) \\ &\leq 2 \sum_{t=1}^T \sum_{\pi \in \Psi} Q_{m(t)}(\pi) \widehat{\text{Reg}}_t(\pi) + \sum_{t=1}^T c_0 \sqrt{\mathbb{E}_W[\mathcal{A}^*(W)]} / \rho_{m(t)} \\ &\leq (2 + c_0) \sqrt{\mathbb{E}_W[\mathcal{A}^*(W)]} \sum_{t=1}^T \frac{1}{\rho_{m(t)}} \\ &\leq (2 + c_0) \sqrt{\mathbb{E}_W[\mathcal{A}^*(W)]} \sum_{m=1}^{\lceil \log T \rceil} \sqrt{\log(2\delta^{-1} |\mathcal{F}^*| \log T) \tau_{m-1} / \eta} \\ &\leq (2 + c_0) \sqrt{\mathbb{E}_W[\mathcal{A}^*(W)]} \sum_{m=1}^{\lceil \log T \rceil} \sqrt{\log(2\delta^{-1} |\mathcal{F}^*| \log T) \tau_{m-1} / \eta} \\ &\leq (2 + c_0) \sqrt{\mathbb{E}_W[\mathcal{A}^*(W)] \log(2\delta^{-1} |\mathcal{F}^*| \log T) \sum_{m=1}^{\lceil \log T \rceil} \tau_{m-1} / \eta} \\ &\leq (2 + c_0) \sqrt{\mathbb{E}_W[\mathcal{A}^*(W)] \log(2\delta^{-1} |\mathcal{F}^*| \log T) T / \eta}. \end{aligned}$$

□

C.11 Proof of Theorem 4.4

Proof. We first consider $|\mathcal{W}| < \infty$. Since the agent has knowledge about causal bound, any function in $\mathcal{F} - \mathcal{F}^*$ can not be the true reward function. For any given context w , the set that the optimal arm will be in is $\mathcal{A}^*(w)$. For any algorithm \mathbf{A} , let \mathbf{A}_w be the induced algorithm of \mathbf{A} when w occurs. Namely, the agent has access to a function space $\mathcal{F}_w = \{f(w, \cdot) | \forall f \in \mathcal{F}^*\}$ and an action set $\mathcal{A}^*(w)$.

From the minimax theorem 5.1 in Agarwal et al. (2012), we know that there exists a contextual bandit instance such that the regret of \mathbf{A}_w is at least $\sqrt{|\mathcal{A}^*(w)| T_w \log |\mathcal{F}_w|} = \sqrt{|\mathcal{A}^*(w)| T_w \log |\mathcal{F}^*|}$, where T_w is the number of occurrence of w . Hence,

$$\begin{aligned} \text{Reg}(T) &\geq \sum_{w \in \mathcal{W}} \sqrt{|\mathcal{A}^*(w)| T_w \log |\mathcal{F}^*|} \\ &\geq \sqrt{\sum_{w \in \mathcal{W}} |\mathcal{A}^*(w)| T_w \log |\mathcal{F}^*|}. \end{aligned}$$

and thus

$$\begin{aligned}
\limsup_{T \rightarrow \infty} \frac{\text{Reg}(T)}{\sqrt{T}} &\geq \sqrt{\sum_{w \in \mathcal{W}} |\mathcal{A}^*(w)| \log |\mathcal{F}^*| \cdot \limsup_{T \rightarrow \infty} \frac{T_w}{T}} \\
&= \sqrt{\sum_{w \in \mathcal{W}} |\mathcal{A}^*(w)| \log |\mathcal{F}^*| \mathbb{P}(W = w)} \\
&= \sqrt{\mathbb{E}_W[|\mathcal{A}^*(W)|] \log |\mathcal{F}^*|}.
\end{aligned}$$

Now assume $|\mathcal{W}| = \infty$. Thanks to Glivenko-Cantelli theorem, the empirical distribution converges uniformly to the true reward distribution. We conclude the proof by applying the dominated convergence theorem and the Fubini's theorem, because $\mathcal{A}^*(w)$ is uniformly bounded by $|\mathcal{A}|$. \square

C.12 Proof of Theorem 4.7

Since any function outside \mathcal{F} cannot be the true reward function, we can take the same steps in the proof of Theorem 4.5. One can simply replace W as W and U in the proof and obtain the final results.

D Related Materials

Definition D.1 (*Back-Door Criterion*) *Given an ordered pair of variables (X, Y) in a directed acyclic graph \mathcal{G} , a set of variables \mathbf{Z} satisfies the back-door criterion relative to (X, Y) , if no node in \mathbf{Z} is a descendant of X , and \mathbf{Z} blocks every path between X and Y that contains an arrow into X .*

Definition D.2 (*d-separation*) *In a causal diagram \mathcal{G} , a path \mathcal{P} is blocked by a set of nodes \mathbf{Z} if and only if*

1. \mathcal{P} contains a chain of nodes $A \leftarrow B \leftarrow C$ or a fork $A \rightarrow B \leftarrow C$ such that the middle node B is in \mathbf{Z} (i.e., B is conditioned on), or
2. \mathcal{P} contains a collider $A \leftarrow B \rightarrow C$ such that the collision node B is not in \mathbf{Z} , and no descendant of B is in \mathbf{Z} .

If \mathbf{Z} blocks every path between two nodes X and Y , then X and Y are d-separated conditional on \mathbf{Z} , and thus are independent conditional on \mathbf{Z} .

If X is a variable in a causal model, its corresponding intervention variable I_X is an exogenous variable with one arrow pointing into X . The range of I_X is the same as the range of X , with one additional value we can call “off”. When I_X is off, the value of X is determined by its other parents in the causal model. When I_X takes any other value, X takes the same value as I_X , regardless of the value of X 's other parents. If X is a set of variables, then I_X will be the set of corresponding intervention variables. We introduce the following do-calculus rules proposed in Pearl (2009).

Rule 1 (Insertion/deletion of observations)

$$\mathbb{P}(\mathbf{Y}|do(\mathbf{x}), \mathbf{Z}, \mathbf{W}) = \mathbb{P}(\mathbf{Y}|do(\mathbf{x}), \mathbf{W})$$

if \mathbf{Y} and $I_{\mathbf{Z}}$ are d-separated by $\mathbf{x} \cup \mathbf{W}$ in \mathcal{G}^* , the graph obtained from \mathcal{G} by removing all arrows pointing into variables in \mathbf{x} .

Rule 2 (Action/observation exchange)

$$\mathbb{P}(\mathbf{Y}|do(\mathbf{x}), do(\mathbf{Z}), \mathbf{W}) = \mathbb{P}(\mathbf{Y}|do(\mathbf{x}), \mathbf{Z}, \mathbf{W})$$

if \mathbf{Y} and $I_{\mathbf{Z}}$ are d-separated by $\mathbf{x} \cup \mathbf{Z} \cup \mathbf{W}$ in \mathcal{G}^\dagger , the graph obtained from \mathcal{G} by removing all arrows pointing into variables in \mathbf{x} and all arrows pointing out of variables in \mathbf{z} .

Rule 3 (Insertion/deletion of actions)

$$\mathbb{P}(\mathbf{Y}|do(\mathbf{x}), do(\mathbf{Z}), \mathbf{W}) = \mathbb{P}(\mathbf{Y}|do(\mathbf{x}), \mathbf{W})$$

if \mathbf{Y} and $I_{\mathbf{Z}}$ are d-separated by $\mathbf{x} \cup \mathbf{W}$ in \mathcal{G}^* , the graph obtained from \mathcal{G} by removing all arrows pointing into variables in \mathbf{x} .